

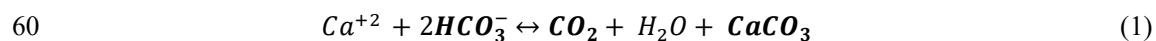




## 31 1. Introduction

32 To mitigate the impact of excess carbon dioxide (CO<sub>2</sub>), humans need to reduce CO<sub>2</sub>  
33 emissions and remove CO<sub>2</sub> from the atmosphere. According to the IPCC, in the 8 years since the  
34 Paris Agreement, global efforts to reduce greenhouse gas emissions are still not on track to avoid  
35 surpassing the 1.5 °C threshold of temperature increase by the end of the century (UNFCCC,  
36 2022). Since reducing CO<sub>2</sub> emissions may not be sufficient to meet the 2015 Paris Agreement  
37 Goals (National Academies of Sciences, 2022), strategies for marine Carbon Dioxide Removal  
38 (mCDR) are being investigated to aid in the uptake and storage of CO<sub>2</sub>. The Earth has balanced  
39 its own carbon storage and acidity on geological timescales (i.e., 100-1000 ka) through mineral  
40 weathering and mineral precipitation. While there may be enough calcium carbonate (CaCO<sub>3</sub>) in  
41 ocean sediments to neutralize all anthropogenic CO<sub>2</sub> (Archer, 1996; Sulpis et al., 2018), this  
42 recovery could take >10,000 years (Zachos et al., 2005). Ocean Alkalinity Enhancement (OAE)  
43 is a mCDR method that can speed up the process of oceanic CO<sub>2</sub> uptake for human relevant  
44 timescales. A thorough assessment of the scientific background and considerations for various  
45 forms of OAE has been presented in Renforth & Henderson (2017). The proposed risks and co-  
46 benefits of increasing surface ocean alkalinity based on different deployment strategies have  
47 been theorized in Bach et al. (2019).

48 There are still many technical challenges to overcome before Ocean Alkalinity Enhancement  
49 can be scaled to remove gigatons of CO<sub>2</sub> (Eisaman et al., 2023; Renforth, 2025). We need to  
50 understand what will happen to ocean chemistry and ecosystems if certain types and amounts of  
51 alkalinity enter the ocean purposefully. The successful long-term sequestration of CO<sub>2</sub> relies on  
52 many factors – the rate of air-sea gas exchange, the loss of alkalinity to re-precipitation of  
53 carbonate minerals or even the loss of an unequilibrated plume as it subducts below the surface  
54 (Lunstrum et al., 2025). Increasing alkalinity could change the cycling of inorganic carbon in the  
55 ocean by increasing the likelihood of calcium carbonate precipitation and thereby affecting the  
56 associated organic carbon cycling pumps (Falkowski et al., 2000; Ridgwell and Zeebe, 2005;  
57 Riebesell et al., 2000; Zondervan et al., 2001). Limiting secondary precipitation of CaCO<sub>3</sub> is  
58 important for OAE because there is rerelease of CO<sub>2</sub> from the precipitation of CaCO<sub>3</sub> (Eq. 1) –  
59 which reduces the efficiency of OAE.





61

62 Another potential outcome of OAE is for organic matter to be ballasted to the deep ocean by  
63 aggregating on newly formed particulate inorganic carbon (PIC) (Riebesell et al., 2009). The  
64 natural global production of particulate organic carbon (POC) is known to be 4-10 times higher  
65 than PIC production (Barker et al., 2006); although this ratio is highly variable in time and space  
66 (Berelson et al., 2007; Dunne et al., 2007). Renforth & Henderson, (2017) hypothesized that if  
67 the POC production remains higher than PIC production even under OAE, then the CO<sub>2</sub>  
68 emissions from CaCO<sub>3</sub> production by marine calcifiers could be offset. This highlights the need  
69 for us to assess when enhanced calcification after OAE will contribute to CO<sub>2</sub> production or if it  
70 might further sequester organic carbon by enhancing POC production or by aggregating and  
71 ballasting POC via enhanced PIC (Bach et al., 2019).

72 Given the variety of compounds available to increase alkalinity (Renforth and Henderson,  
73 2017), their composition and deployment style will determine the magnitude of change in Omega  
74 (the saturation state) and likelihood of CaCO<sub>3</sub> precipitation. This applies to both the near field  
75 impacts at the point of injection and the far field impacts after the alkalinity has been dispersed.  
76 Thus far, some studies have characterized instances of short term (<5 days) (Hartmann et al.,  
77 2023; Hashim et al., 2025; Subhas et al., 2022), and longer term (~20 days) (Moras et al., 2022,  
78 2024; Paul et al., 2024; Suitner et al., 2024) increased carbonate mineral precipitation by  
79 showing the loss of alkalinity and DIC following OAE. These examples come from natural  
80 waters around Spain, North Pacific, North Atlantic gyres, and Australian coastal waters. In  
81 Norway, in water between 10-15°C one maximum threshold for NaOH addition before the onset  
82 of secondary precipitation has been reported at ~1500 μmol kg<sup>-1</sup> ( $\Omega_{\text{aragonite}} \sim 22$ ) after which  
83 dilution of the water mass must occur within 15 days. In the same study, NaHCO<sub>3</sub>/Na<sub>2</sub>CO<sub>3</sub>  
84 addition was stable up to  $\Omega_{\text{aragonite}} \sim 20$ , with no observed precipitation without dilution for 20  
85 days (Suitner et al., 2024). Yet, in the Sargasso Sea, in water around 27°C secondary  
86 precipitation was observed even at an addition of 500 μmol kg<sup>-1</sup> NaOH ( $\Omega_{\text{aragonite}} \sim 11$ ) within 5  
87 days (Hashim et al., 2025). With grain feedstock added to Australian waters at 21°C, secondary  
88 precipitation was not observed for up to 25 days only after increasing TA by 250 μmol kg<sup>-1</sup>  
89 ( $\Omega_{\text{aragonite}} \sim 5$ ) with Ca(OH)<sub>2</sub> (Moras et al., 2022). OAE experiments conducted with cultures of  
90 coccolithophores report negligible changes to calcification rates after additions of bicarbonate



91 and calcium raise  $\Omega_{\text{aragonite}}$  to 15 (Gately et al., 2023). These prior experiments leave ambiguity  
92 in extrapolating the precipitation thresholds of various feedstocks to waters in other regions.

93 To this steadily growing body of research, we present the changes of particulate organic and  
94 inorganic carbon inventory during 4-day OAE experiments conducted using coastal California  
95 waters from Los Angeles Harbor. The waters offshore from Los Angeles are richly characterized  
96 by decades of regional studies (<https://dornsife.usc.edu/spot/publications-and-projects/>,  
97 <https://calcofi.org/publications/peer-reviewed-publications/>). Yet waters from within LA Harbor  
98 contain blends of offshore ecosystems modified by nearshore processes. In our study, we use  
99 three different approaches of elevating  $\Omega_{\text{aragonite}}$  by: (i) increasing pH (using two different bases)  
100 and (ii) adding  $\text{Ca}^{+2}$  coupled with increasing the total dissolved inorganic carbon (DIC). In  
101 constraining the resultant changes to the amount of PIC, POC and DOC production, we conduct  
102 a carbon budget analysis that helps define how alkalinity may change the natural cycling of  
103 organic and inorganic carbon.

## 104 **2. Study Area & Methods**

### 105 **2.1 Study Area**

106 With the exception of some short term experiments conducted on Catalina Island, all  
107 other experiments were conducted with water collected from Los Angeles Harbor, at AltaSea  
108 Marine Center (33° 43' 33.64" N, 118° 16' 11.999" W). This region exchanges seawater with the  
109 Southern California Bight, which is a part of the California Current System. The microbial  
110 community structure in the Port of Los Angeles in the summer is dominated by diatoms, pico-  
111 eukaryotes, and heterotrophic bacteria. Dinoflagellates, *Synechococcus*, and photosynthetic  
112 nanoplankton are in less abundance. In the fall, the carbon biomass shifts to the following in  
113 order of abundance: Bacteria > Picoeukaryotes > *Synechococcus* > Diatoms ~ Pico  
114 nanoplankton > Dinoflagellates; these proportionally decrease in the winter when Diatoms  
115 become the dominant species again (Bialonski et al., 2016; Caron et al., 2017; Connell et al.,  
116 2017). Regardless of the season, the carbon biomass is higher in the Port compared to the costal  
117 San Pedro Ocean Time series station (~17 km offshore) or in the marine protected area near  
118 Santa Catalina Island (~45 km offshore) (Connell et al., 2017).



119 Alkalinity perturbation experiments were conducted with 5 L, Nalgene PETG bottles  
 120 suspended 1 m below the water surface off a dock at AltaSea. Surface seawater conditions  
 121 (salinity, temperature, and sunlight exposure) during each experiment are recorded in Table 1.  
 122 Temperature (°C) and Light Intensity (lux) were measured with HOBO™ Temperature and Light  
 123 Loggers, and the lux was converted to photosynthetic photon flux density ( $\mu\text{mol photons m}^{-2} \text{s}^{-1}$ )  
 124 by multiplying lux with the standard conversion factor of sunlight (0.0185). Salinity was  
 125 measured with a refractometer (units reported in ppt).

126 **Table 1. Ambient Sea Surface Conditions during each Experimental Deployment.**

	<b>Start Date</b>	<b>Sea Surface Temperature (°C)</b>	<b>Salinity (PPT)</b>	<b>Light (<math>\mu\text{mol m}^{-2} \text{s}^{-1}</math>)</b>
<b>CaCl<sub>2</sub> + NaHCO<sub>3</sub></b> (+500 $\mu\text{mol kg}^{-1}$ )	06-24-24	16.4 – 22.3	35	0 – 540
	07-15-24	17.4 – 24.5	35	0 – 605
<b>NaOH</b> (+500 $\mu\text{mol kg}^{-1}$ )	06-17-24	17.2* - 21.1*	35	0 – 640
	07-22-24	15.8 – 20.8	35	0 – 605
<b>CaO</b> (+500 $\mu\text{mol kg}^{-1}$ )	11-18-24	13.7* - 14.7*	35	0 – 400
	01-27-25	13.5 – 20.8	35	0 – 470
<b>CaO</b> (+1000 $\mu\text{mol kg}^{-1}$ )	11-04-24	14.1 – 22.01	35	0 – 620

127 \*Data taken from *NOAA Tides & Currents* from Station #9410840 Santa Monica, CA. All other data  
 128 measured from the AltaSea dock side water at 1 m water depth.

129

130 **2.2 Alkalinity Types**

131 In this study we induce an alkalinity perturbation that simulates two different methods of  
 132 OAE, (1) Base Addition: where a strong base is delivered to the surface of the ocean and is  
 133 intended to increase oceanic uptake of atmospheric CO<sub>2</sub> by disrupting the pH/charge balance. To  
 134 simulate this, we use two common bases, Sodium Hydroxide (NaOH, J. T. Baker, New Jersey),  
 135 and Lime (CaO, Sigma-Aldrich, Missouri). The other method considered here is (2) the product  
 136 of limestone weathering, purposeful weathering is called accelerated weathering of limestone,  
 137 AWL (Dong et al., 2025; Kheshgi, 1995; Rau and Caldeira, 1999). When this occurs with



138 seawater, the products are enriched in  $\text{Ca}^{+2}$  ion and  $\text{HCO}_3^-$  ions. We mimic AWL with the  
139 addition of Calcium Chloride ( $\text{CaCl}_2$ , Sigma-Aldrich, Missouri) and Sodium Bicarbonate  
140 ( $\text{NaHCO}_3$ , Sigma-Aldrich, Missouri) with a molar ratio of Ca: $\text{HCO}_3$  of 1:2.

141 Since we were most concerned with assessing the impact of alkalinity at specific  
142 dosages/concentrations, we wanted the alkalinity to be fully dissolved, and we avoided  
143 introducing any particles into the incubations. Also, aqueous alkalinity delivery is currently  
144 considered a favorable delivery method for OAE projects (Cai and Jiao, 2022; Savoie et al.,  
145 2025). We created dissolved stock solutions of each alkalinity type ( $\text{NaOH}$ ,  $\text{CaO}$ ,  $\text{CaCl}_2$ ,  
146  $\text{NaHCO}_3$ ) with minimal exposure to the atmosphere. A solid salt or base was precisely weighed,  
147 transferred to a pre-weighed volumetric flask, the flask was filled with Milli-Q water, and no  
148 headspace remained. After all solids were dissolved, the solution was siphoned through a  $0.2 \mu\text{m}$   
149 GF/F filter into an evacuated gas impermeable foil bag (Supelco, Pennsylvania) for storage. We  
150 took subsamples for alkalinity and dissolved inorganic carbon (DIC) to calculate the final  
151 concentrations of the stock solutions and precisely dosed our incubations according to these  
152 measurements to achieve the alkalinity enrichments desired. In all  $\text{CaO}$  experiments, the DIC  
153 was immediately lowered (by  $<2\%$ ) due to an expected dilution by the lower salinity stock  
154 solution (we add 100-160 mL of stock depending on the desired concentration). Alkalinity was  
155 measured with an open-system Gran titration method at  $25^\circ\text{C}$  (details in (Lunstrum and  
156 Berelson, 2022; Subhas et al., 2015)).

### 157 **2.3 Experimental Set Up**

158 There is long standing discourse on whether bottle experiments mimic natural conditions  
159 enough to be useful to answer questions of “ecosystem impact” (Daehler and Strong, 1996;  
160 Fraser and Keddy, 1997; Giesy, 1980; Ives et al., 1996; Lawton et al., 1993; Stachowski-  
161 Haberkorn et al., 2008). There are many experimental design factors that can influence the  
162 community assemblage, such as: material used for the structure, microcosm volume, filling  
163 mechanism, mixing, replication, carbonate chemistry, exclusion of larger organisms, and wall  
164 surface growth (Riebesell et al., 2010). Since the chapter on laboratory and mesocosm  
165 experimental design written by Iglesias-Rodríguez et al. (2023) in State of the Planet’s “Guide to  
166 Best Practices in Ocean Alkalinity Enhancement Research” details how different styles of lab  
167 experiments are very useful – we follow their recommendations. We determined the best design



168 to answer our questions for this study were sacrificial replication 4-day bottle incubation  
169 experiments. We intended to maintain a closed system experiment to constrain the carbon budget  
170 by eliminating gas exchange as a potential variable for this study. This can be an analog for water  
171 that may temporarily lose contact with the atmosphere, e.g. when waters mix deeper into surface  
172 ocean or for times when gas exchange is minimal.

173 We collected seawater for each experimental treatment by pumping from 1 m below the  
174 surface from a dock at AltaSea, in the Los Angeles Harbor. The water passed through a 250  $\mu\text{m}$   
175 mesh (to remove large grazers) (Carter et al., 2005; de la Broise and Palenik, 2007) and the  
176 bottles were filled in a ‘round robin’ manner to promote homogeneity between bottles filled at  
177 different times (~20 bottles were filled < 20 mins). Once all bottles were full, with no headspace,  
178 half were randomly selected to receive a dosage of alkalinity (NaOH, CaO, or  $\text{CaCl}_2 +$   
179  $\text{NaHCO}_3$ ). Only one treatment experiment was conducted per week; hence, we can only compare  
180 each alkalinity type to its respective control (no addition of alkalinity). Sampling occurred on  
181 days 0, 2, and 4 with three bottle replicates per time point.

182 We also filled and added alkalinity to 2 bottles that were incubated devoid of light as well as  
183 2 dark controls (wrapped in black tape, See Fig. 1). Results and discussion of all dark bottle  
184 experiments appear in the Supplemental Information. All treatment bottles were given a dose of  
185 alkalinity on Day 0, some were immediately sampled, others left in the water column to  
186 experience natural changes in temperature and light condition until their sampling day. While  
187 dosing the bottles, we added a  $^{13}\text{C}$  tracer (controls and treatments) in the form of  $\text{NaH}^{13}\text{CO}_3$   
188 (Sigma Aldrich, Missouri). This spike only changed the alkalinity by 2  $\mu\text{mol kg}^{-1}$  but increased  
189 the  $\delta^{13}\text{DIC}$  signal to a couple hundred per mil– the purpose of this was to increase the sensitivity  
190 of our measurements for our carbon budget analysis.

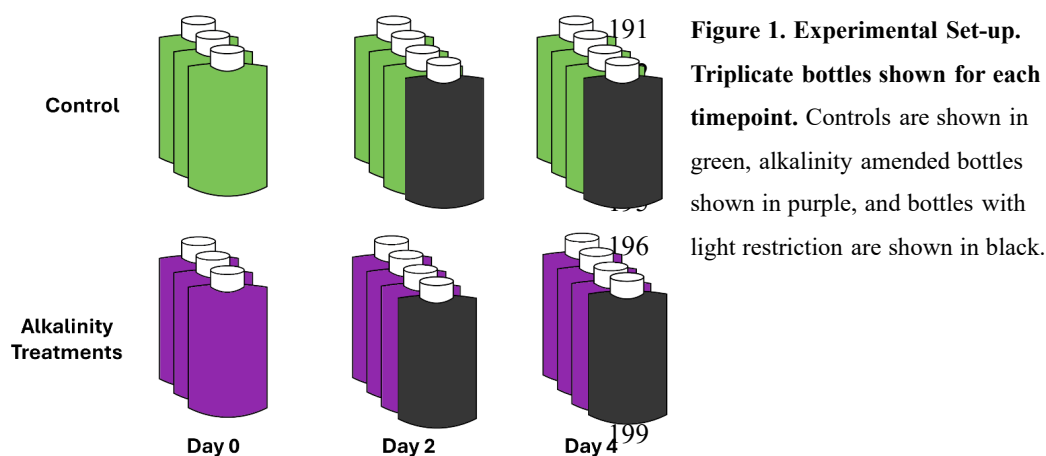


**Figure 1. Experimental Set-up.** Triplicate bottles shown for each timepoint. Controls are shown in green, alkalinity amended bottles shown in purple, and bottles with light restriction are shown in black.

200 **2.4 Sample Processing**

201 Bottles pulled out of the ocean were transported back to the lab (on ice) on their sampling  
 202 day and weighed to track water that was used for sub-sampling. Bottles were gently inverted 5  
 203 times and then opened to measure temperature (°C) with a probe and dissolved oxygen ( $\mu\text{mol kg}^{-1}$ )  
 204 with PreSens Optical Oxygen Sensor Spots that were attached to each bottle. The oxygen  
 205 measurements were corrected to the mean temperature recorded by the in situ HOBOTM Loggers.  
 206 The first 250 mL of sample water was filtered through a 25 mm 0.7  $\mu\text{m}$  glass fiber filter  
 207 (Whatmann GF/F). A portion of the filtrate was collected for dissolved inorganic carbon  
 208 (duplicates of 5 mL), alkalinity (15 mL), nutrients (15 mL), dissolved organic carbon (40 mL),  
 209 and 50 mL for archival purposes. This GF/F was wrapped in aluminum foil and placed in a  
 210 freezer (-20 °C) for later Chl a analysis (< a month) (using a Turner Trilogy Fluorometer and the  
 211 EPA SOP LG405.v11 for ‘Chlorophyll-A Non-Acidification Method’ (U.S. EPA, 2021)). One  
 212 liter was filtered for future genomic analyses not discussed in this paper, on Supor 0.2  $\mu\text{m}$  47  
 213 mm PES filters, and stored at -80 °C. The remaining (4.5 L) seawater was filtered (detailed in  
 214 Section 2.5.2) for particulate organic and inorganic carbon.

215

216 **2.5 Measurements for Carbon Budget**

217 A carbon budget for each bottle was created by assessing the total concentration of carbon in  
 218 the dissolved and particulate pools. Carbonate system parameters were derived from Total  
 219 Alkalinity and DIC measurements (discussed below) using CO2Sys.v3 (Pierrot et al., 2021)



220 (Parameters: pH Scale = Total Scale (mol per kg-SW), CO<sub>2</sub> Constants = (Dickson and Millero,  
221 1987), KSO<sub>4</sub> = (Dickson, 1990), KF = (Perez and Fraga, 1987), Boron = (Lee et al., 2010)).  
222  $\Omega_{\text{aragonite}}$  values for treatments with added Ca<sup>+2</sup> (CaO & Dissolved Limestone Experiments) were  
223 calculated by multiplying the [CO<sub>3</sub><sup>2-</sup>] output from CO2Sys and [Ca<sup>+2</sup>] accounting for the  
224 increased Ca. All calculations use  $K_{\text{sp}}'$  for Aragonite in seawater ( $K_{\text{sp}}' = 10^{-6.19}$ ). All other  
225  $\Omega_{\text{aragonite}}$  values derived from CO2Sys scale [Ca<sup>+2</sup>] to salinity.

### 226 **2.5.1 Dissolved Carbon Phases**

227 Samples for Dissolved Inorganic Carbon (DIC) were collected in pre-evacuated 12 mL  
228 Labco Exetainers and immediately placed at 4 °C for storage until analysis (< 1 week). For  
229 analysis, samples were acidified with 2 mL of 10 % H<sub>3</sub>PO<sub>4</sub> (Spectrum Chemicals, Gardena,  
230 California) and the evolved CO<sub>2</sub> was analyzed by a Picarro G2121-i Cavity Ring Down  
231 Spectrometer (as detailed in (Subhas et al., 2015). Optical grade calcite, with a known <sup>13</sup>C value  
232 (2.47 ‰) was used to create a standard curve (ppmCO<sub>2</sub> per mg of CaCO<sub>3</sub>) and a certified  
233 reference material (CRM-Batch 214) generated by Andrew Dickson's Lab at SIO, UCSD was  
234 used to correct all the final DIC concentrations. The total CO<sub>2</sub> standard curve produced with the  
235 Automate Sample Delivery System + Picarro CRDS had an  $R^2 = 0.9999 \pm 0.0001$  and slope  
236 variability = 1.5 % for all runs in this dataset. Replicate CRM samples provided a measure of  
237 precision,  $\pm 20 \mu\text{mol kg}^{-1}$ . The isotopic values of replicate standards were within  $\pm 0.2 \text{ ‰}$ .

238 Samples for Dissolved Organic Carbon (DOC) were collected in 40 mL pre-combusted  
239 amber glass vials, acidified to 0.1 % v/v with concentrated hydrochloric acid (ACS grade,  
240 Supelco, Massachusetts), and placed in cold storage (4 °C) until analysis. The samples were run  
241 on a Shimadzu TOC-L Analyzer (NPOC method; Injection volume = 150  $\mu\text{L}$ ; No. of Injections:  
242 Best 4 of 5; Max Variance of Replicates: 2.00 %). Within a run the standard curve had an  $R^2 =$   
243  $0.9998 \pm 0.0002$ , between runs the reproducibility of the slope had 16.5 % error. Samples were  
244 initially purged with CO<sub>2</sub>-free compressed air to remove inorganic carbon, combusted in a  
245 furnace via catalytic oxidation, and the generated CO<sub>2</sub> was measured by an infrared gas analysis.  
246 Standards for organic carbon were made with Oxalic Acid (dried at 70 °C for 2 hr), and CRMs  
247 from the Hansell Lab (University of Miami, RSMAS) were used to correct final concentrations  
248 (DSR Batch 22 Lot # 10-22).

### 249 **2.5.2 Particulate Carbon Phases**



250 Roughly 4.5 L of seawater was filtered on 1-2 filters (0.7  $\mu\text{m}$  47mm Whatman GF/F) for  
251 particulate inorganic carbon (PIC) and particulate organic carbon (POC) analyses. After  
252 filtration,  $\sim 10$  mL of buffered DI water (NaOH added to Milli-Q, pH 9) was used to rinse any  
253 residual seawater, and then filters were placed in the oven to dry overnight (60  $^{\circ}\text{C}$ ). Filters were  
254 hole punched (diameter = duplicates of 6-12.5 mm); the hole punched fractions (2-8 % of total  
255 filtered area) were wrapped in tin foil capsules (9 x 5 mm) for combustion in a CosTech  
256 Elemental Analyzer – which is connected to the Picarro for  $\text{CO}_2$  and  $^{12}\text{C}/^{13}\text{C}$  analysis. This  
257 analysis of Total Carbon had a reproducibility of  $\pm 1$  %. The remaining fraction of the filters  
258 were rolled and placed into Labco Exetainers – these samples were acidified with 5 mL 10 %  
259  $\text{H}_3\text{PO}_4$  and the evolved  $\text{CO}_2$  measured similarly to DIC described above. Particulate Organic  
260 Carbon (POC) was calculated by subtracting the PIC ( $\mu\text{gC L}^{-1}$ ) concentration from the Total  
261 Carbon ( $\mu\text{gC L}^{-1}$ ) calculated for the whole filtered area.

## 262 **2.6 Data Visualization and Statistical Analysis**

263 Statistical analysis and data visualization was conducted in R and R Studio version 4.5.1.  
264 Means and standard deviations for each treatment by time point were generated using the  
265 data\_summary function. Triplicate values were averaged, but data points that were found outside  
266 of three standard deviations from the mean were flagged as outliers and not included in the  
267 statistical analysis (Pukelsheim, 1994). The dataset was analyzed with two statistical approaches:  
268 (i) To test whether the effect of alkalinity addition had a statistically significant impact on PIC,  
269 POC, DOC and Chl a over time, we used a linear model with an interaction term and assessed if  
270 the p-value on the interaction term (i.e., the difference between the slopes of the control and the  
271 treatment) was statistically significant (significance threshold  $\alpha = 0.05$ ) (results summarized  
272 Table 4). (ii) Since the previous method assumes linear relationships and normally distributed  
273 data (which may apply to some but not all variables) we also used a nonparametric two way  
274 ANOVA (Analysis of Variance) – Scheirer Ray Hare test – to assess the impact of alkalinity  
275 addition on the Control and Treatment groups (significance threshold  $\alpha = 0.05$ ) (results  
276 summarized in Table 5). The implications of these tests and any statistically significant responses  
277 are summarized in the context of ecological variability in the Results and Discussion sections.

## 278 **3. Results**

### 279 **3.1 Simulating AWL with $\text{CaCl}_2 + \text{NaHCO}_3$ Addition**



### 280 3.1.1 Observing Short Term Impacts at Extremely Low Alkalinity Additions

281 With the intent to recreate an alkalinity impact condition that resembles extremely high  
 282 dilution of bicarbonate after a few hours, we conducted an experiment where the presumed  
 283 outflow of alkalinity from a shipping vessel of  $5000 \mu\text{mol kg}^{-1}$  was diluted by different  
 284 proportions; 150, 300, and 600 x (Table 2) based on dilution calculations presented by Dong et  
 285 al., (2025). These incubations that lasted 3 hours and were conducted on Catalina Island at the  
 286 USC Dornsife Wrigley Marine Science Center ( $33^\circ 26' 40.52'' \text{N}$ ,  $118^\circ 28' 47.787'' \text{W}$ ).

287 In the least diluted sample, the seawater alkalinity changes from  $2223 \pm 2 \mu\text{mol kg}^{-1}$  to  
 288  $2233 \pm 2 \mu\text{mol kg}^{-1}$  but there is not a statistically significant impact on the concentrations of  
 289 particulate inorganic or organic carbon ( $p > 0.05$ ). Since we saw no impact on PIC or POC at  
 290 such small changes in alkalinity (at what could be realistic deployment concentrations after  
 291 several hours of mixing), we focused the rest of the paper on experiments that perturb the  
 292 alkalinity by larger amounts (25-50 %) and longer durations (2-4 days). All the following  
 293 experiments were conducted with water collected and incubated at AltaSea in LA Harbor.

294 **Table 2. Summary of low concentration alkalinity amendments.**

Treatment	Alkalinity ( $\mu\text{mol kg}^{-1}$ )	DIC ( $\mu\text{mol kg}^{-1}$ )	$\Omega_{\text{aragonite}}$	pCO <sub>2</sub> ( $\mu\text{atm}$ )	PIC ( $\mu\text{g L}^{-1}$ )	POC ( $\mu\text{g L}^{-1}$ )
Control	$2223 \pm 2$	$2000 \pm 1$	$2.53 \pm 0.02$	$585 \pm 5$	$7.1 \pm 0.2$	$68.4 \pm 7.7$
1:600	$2232 \pm 5$	$2010 \pm 3$	$2.57 \pm 0.08$	$580 \pm 20$	$6.8 \pm 0.2$	$69.0 \pm 9.7$
1:300	$2234 \pm 2$	$2025 \pm 25$	$2.46 \pm 0.2$	$625 \pm 90$	$6.7 \pm 0$	$66.9 \pm 6.7$
1:150	$2233 \pm 2$	$2030 \pm 6$	$2.40 \pm 0.06$	$640 \pm 25$	$7.0 \pm 0.3$	$80.6 \pm 20.5$

295 The treatments are shown as dilution ratios - i.e., the 1:600 treatments received 1 part of a stock alkalinity  
 296 ( $5000 \mu\text{mol kg}^{-1}$ ) per 600 parts of seawater. The reported error is standard deviations between triplicate  
 297 bottles ( $n = 3$ ).

### 298 3.1.2 [Ca<sup>+2</sup>] and [HCO<sub>3</sub><sup>-</sup>] addition: Alkalinity Enhancement~500 $\mu\text{mol kg}^{-1}$

299 We performed two calcium and bicarbonate addition experiments on 24 June 2024 and 15  
 300 July 2024. Alkalinity added in the form of HCO<sub>3</sub><sup>-</sup> increases both alkalinity and DIC in a 1:1 ratio  
 301 – hence, the change in pH relative to the Control is minimal for this treatment (Fig. 2). Over the  
 302 4-day incubation, this treatment resulted in no statistically significant difference in the



303 production of PIC ( $p > 0.05$ , ANOVA and Linear Regression method, see Table 4 & 5), the  
 304  $\Omega_{\text{aragonite}}$  only increases by 0.2 units in both experiments (Table 3). POC in the control (untreated)  
 305 seawater triples by the end of the experiment (Fig. 3), but there is no statistical difference  
 306 between the POC or DOC change in concentration of the control vs. the treatment condition for  
 307 both experiments ( $p > 0.05$ , ANOVA and Linear Regression method). Chl a also shows that  
 308 changes in concentration over time were similar in both the control and the dissolved limestone  
 309 treatment.

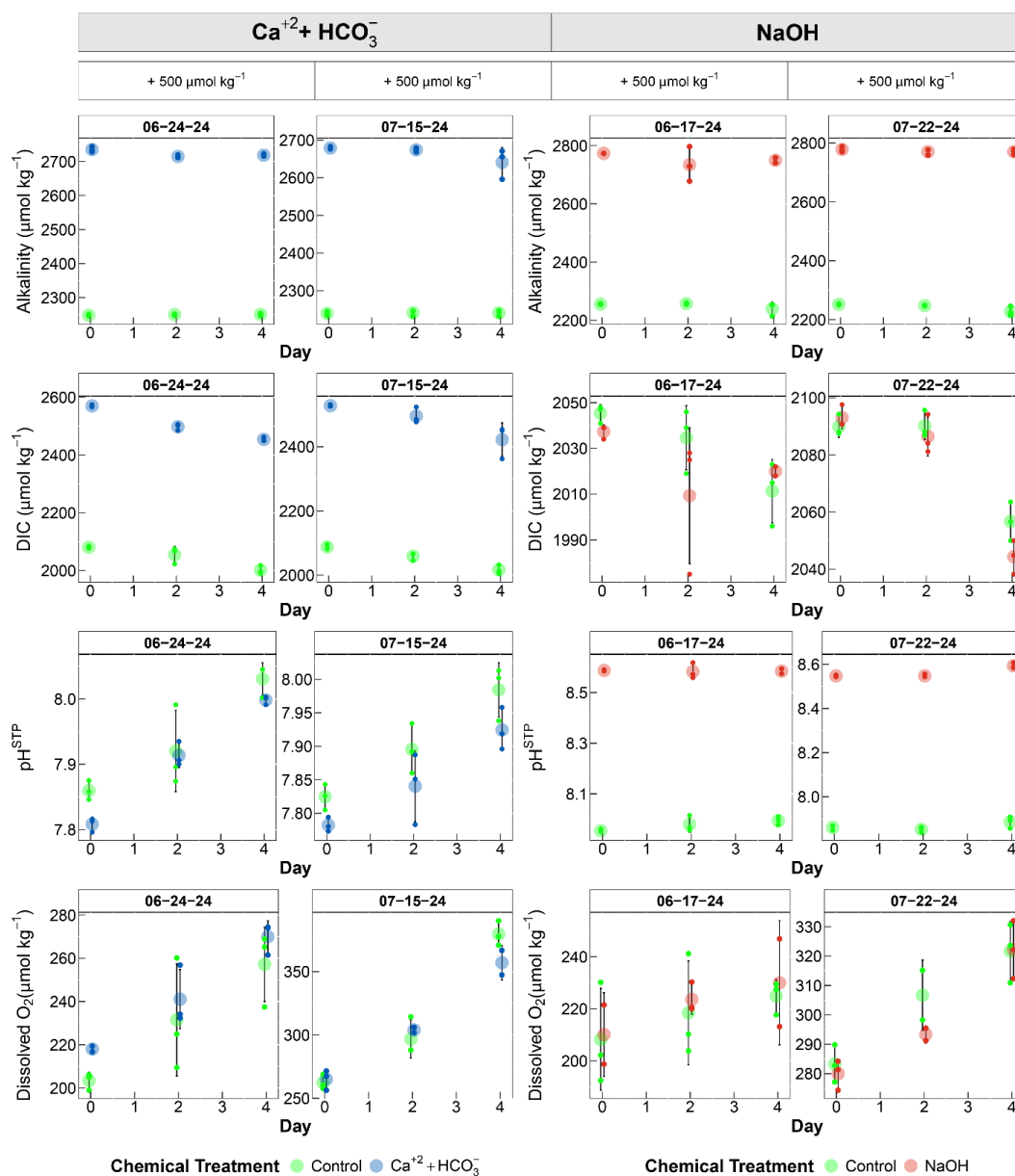
310 **Table 3. Initial Concentrations of Biogeochemical Parameters at Day 0 (Control) of**  
 311 **Experiments**

	Start Date	PIC $\mu\text{gC L}^{-1}$	POC $\mu\text{gC L}^{-1}$	CHL $\mu\text{g L}^{-1}$	DOC $\mu\text{mol kg}^{-1}$	Control $\Omega_{\text{aragonite}}$	Treatment $\Omega_{\text{aragonite}}$
<b>CaCl<sub>2</sub> + NaHCO<sub>3</sub></b> <b>(+500 <math>\mu\text{mol kg}^{-1}</math>)</b>	06-24-24	$3.90 \pm 1.15$	$278 \pm 20$	$2.37 \pm 0.25$	NA	$2.02 \pm 0.06$	$2.28 \pm 0.05$
	07-15-24	$2.51 \pm 0.30$	$209 \pm 18$	$0.60 \pm 0.21$	$117 \pm 15$	$1.88 \pm 0.07$	$2.12 \pm 0.05$
<b>NaOH</b> <b>(+500 <math>\mu\text{mol kg}^{-1}</math>)</b>	06-17-24	$0.95 \pm 0.21$	$366 \pm 33$	$1.82 \pm 0.32$	NA	$2.28 \pm 0.02$	$8.21 \pm 0.04$
	07-22-24	$1.16 \pm 1.02$	$369 \pm 26$	$1.91 \pm 0.40$	$96.1 \pm 12.8$	$1.92 \pm 0.04$	$7.63 \pm 0.07$
<b>CaO</b> <b>(+500 <math>\mu\text{mol kg}^{-1}</math>)</b>	11-18-24	$100.0 \pm 49.3$	$171 \pm 48$	$0.09 \pm 0.02$	$29.2 \pm 1.15$	$1.47 \pm 0.02$	$7.97 \pm 0.23$
	01-27-25	$28.4 \pm 4.53$	$279 \pm 83$	$0.56 \pm 0.07$	$66.2 \pm 2.16$	$1.23 \pm 0.14$	$8.63 \pm 0.16$
<b>CaO</b> <b>(+1000 <math>\mu\text{mol kg}^{-1}</math>)</b>	11-04-24	$4.83 \pm 0.79$	$218 \pm 25$	$0.76 \pm 0.07$	$65.2 \pm 1.59$	$1.81 \pm 0.04$	$13.73 \pm 0.09$

312

313 **3.2 NaOH addition: Alkalinity Enhancement  $\sim 500 \mu\text{mol kg}^{-1}$**

314 Sodium hydroxide additions occurred on 17 June 2024 and 22 July 2024. The addition of  
 315 NaOH increases alkalinity but not DIC which results in a large change in  $\Omega_{\text{aragonite}}$  from  $\sim 2$  to  
 316  $8.21 \pm 0.04$  (06-17-24; pH increases 0.63) and  $7.63 \pm 0.07$  (07-22-24; pH increases 0.71). When  
 317 compared to the control condition, the changes in PIC, POC, DOC, and Chl a in the treatment  
 318 conditions are also not statistically significant (Fig. 3) via either of two statistical analyses  
 319 ( $p > 0.05$ , ANOVA and Linear Regression methods). As with the  $[\text{Ca}^{+2}]$  and  $[\text{HCO}_3^-]$  addition,  
 320 there are certain points in time where the controls diverge from the treatments, but there are no  
 321 consistent trends across multiple variables (i.e., no indication that one group (control/treatment)  
 322 is consistently higher/lower through time).



323

324 **Figure 2. Summary of Water Chemistry from (NaOH and NaHCO<sub>3</sub> + CaCl<sub>2</sub>) Amendment**

325 **Experiments.** Panels are grouped by the alkalinity treatment they received: Controls (green), NaOH (red)

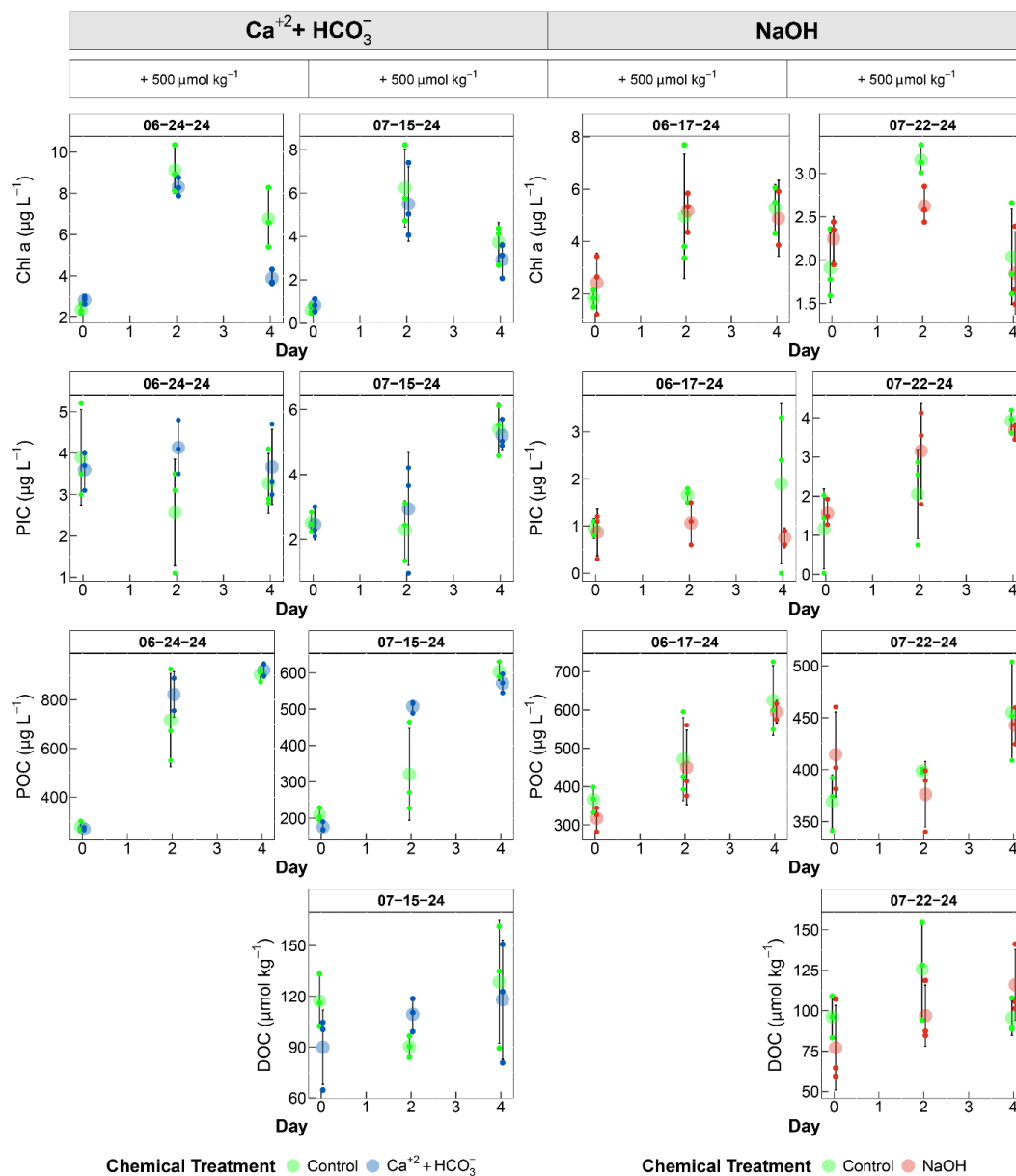
326 and CaCl<sub>2</sub> + NaHCO<sub>3</sub> (blue). The start date of the experiment is listed for reference to differentiate

327 between duplicate experiments. The four variables displayed here are measured Alkalinity (µmol kg<sup>-1</sup>),

328 measured Dissolved Inorganic Carbon (DIC) (µmol kg<sup>-1</sup>), pH calculated from CO2Sys.v3, and dissolved



329 oxygen ( $\mu\text{mol kg}^{-1}$ ). Each plot shows the average of the treatment per timepoint ( $n = 3$ ), and the error bars  
 330 are the standard deviation between the triplicate bottles. Smaller symbols show individual bottles.



331

332 **Figure 3. Four Day Timeseries of Biogeochemical Response to Different Alkalinity Enhancements.**

333 Smaller symbols show individual bottles; larger symbols show the mean. Error bars are the standard



334 deviation between replicates ( $n = 3$ ). The start date of the experiment and the amount of alkalinity added  
335 are included as headers for reference. The variables displayed are Chl a ( $\mu\text{g L}^{-1}$ ), PIC - Particulate  
336 Inorganic Carbon ( $\mu\text{g L}^{-1}$ ), POC- Particulate Organic Carbon ( $\mu\text{g L}^{-1}$ ), and DOC- Dissolved Organic  
337 Carbon ( $\mu\text{mol kg}^{-1}$ ).

### 338 **3.3 CaO Additions**

#### 339 **3.3.1 CaO addition: Alkalinity Enhancement $\sim 1000 \mu\text{mol kg}^{-1}$ (4 November 2024)**

340 The CaO experiment raised the Omega value above the threshold for spontaneous  
341 precipitation of calcium carbonate in seawater ( $\Omega_{\text{aragonite}} > 12$ ,  $\Omega_{\text{calcite}} > 19$  (Marion et al., 2009;  
342 Morse and He, 1993)) according to the references cited. Increasing TA by 1000  $\mu\text{mol/kg}$  raised  
343 the  $\Omega_{\text{aragonite}}$  from  $1.81 \pm 0.04$  to  $13.73 \pm 0.09$  and pH was raised from  $7.85 \pm 0.01$  to  $8.91 \pm 0.01$   
344 (error is standard deviation between replicate bottles). Yet in these incubations, we see no  
345 statistically significant increase in PIC either immediately after CaO addition or throughout the  
346 4-day experiment ( $p > 0.05$ , nonparametric ANOVA and linear analysis, Table 4 & 5). We also  
347 see no statistically significant divergence between the Control bottles and CaO bottles in DOC or  
348 Chl a (nonparametric ANOVA and linear analysis,  $p > 0.05$ ). However, the  $\text{O}_2$  and POC trends  
349 are statistically different than the Control after CaO addition ( $p < 0.05$  with linear analysis,  
350 Table 4). This is the only experiment where we see a statistically significant impact of CaO  
351 addition with a 95% confidence interval. The production of  $\text{O}_2$  is  $70 \pm 20 \mu\text{mol kg}^{-1}$  over 4 days  
352 in the Control, compared to no change in measured  $\text{O}_2$  in the CaO treatment. In the Control, the  
353 POC production increases by  $180 \pm 35 \mu\text{gC L}^{-1}$  ( $\sim 15 \pm 3 \mu\text{mol kg}^{-1}$ ) compared to only a  $70 \pm 40$   
354  $\mu\text{gC L}^{-1}$  ( $\sim 5.8 \pm 3.6 \mu\text{mol kg}^{-1}$ ) increase in the treated waters.

#### 355 **3.3.2 CaO addition: Alkalinity Enhancement $\sim 500 \mu\text{mol kg}^{-1}$ with Higher Ambient PIC**

356 Twice we added CaO to enhance alkalinity by  $500 \mu\text{mol kg}^{-1}$ , similar to the amount of  
357 enhanced alkalinity in the  $[\text{Ca}^{+2}] + [\text{HCO}_3^-]$  and NaOH treatments. In the 18 November 2024  
358 experiment, ambient PIC concentrations were  $\sim 20$  times higher than the ambient PIC ( $5 \pm 5 \mu\text{gC}$   
359  $\text{L}^{-1}$ ) of the experiments described above (Fig. 3 & Fig. 5). We used this opportunity as an analog  
360 to study an alkalinity addition with greater suspended solids – i.e., greater nucleation sites for  
361 secondary precipitation – in a natural seawater environment. The CaO addition raised pH from  
362  $7.75 \pm 0.01$  to  $8.57 \pm 0.01$ , and  $\Omega_{\text{aragonite}}$  from  $1.47 \pm 0.02$  to  $7.97 \pm 0.23$ . We saw no increase in

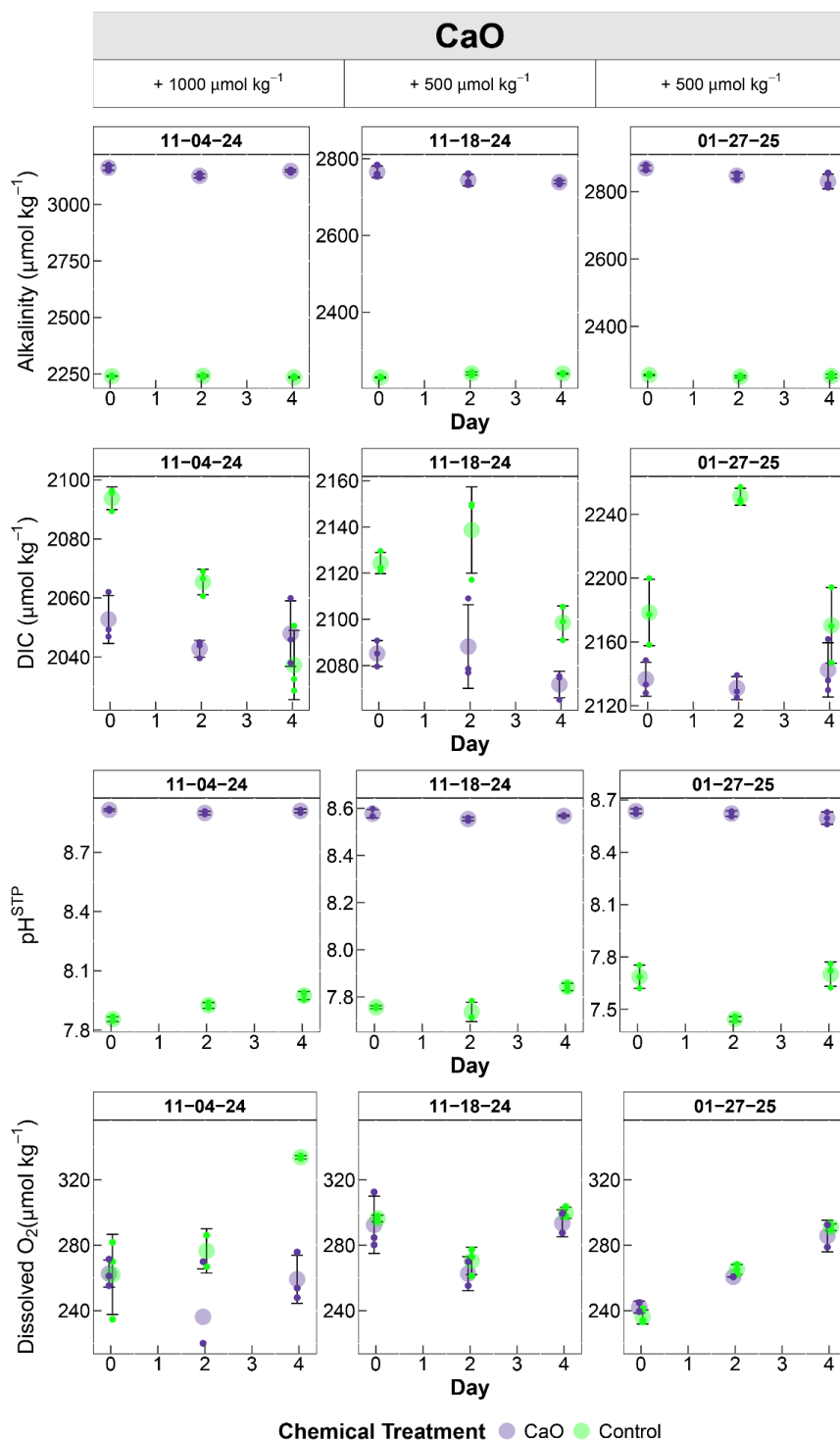


363 PIC formation in the treatment compared to the control. Instead, we observed a loss of PIC  
364 occurring over time in both the control and treated bottles. Chl a, DOC, and dissolved O<sub>2</sub> show  
365 no statistically significant changes over time from the alkalinity addition; POC in the Control  
366 samples is higher than the treatment (Fig. 5), however, Day 0 variability negates any statistically  
367 significant impact.

### 368 **3.3.3 CaO Addition: Alkalinity Enhancement ~500 μmol kg<sup>-1</sup> (27 January 2025)**

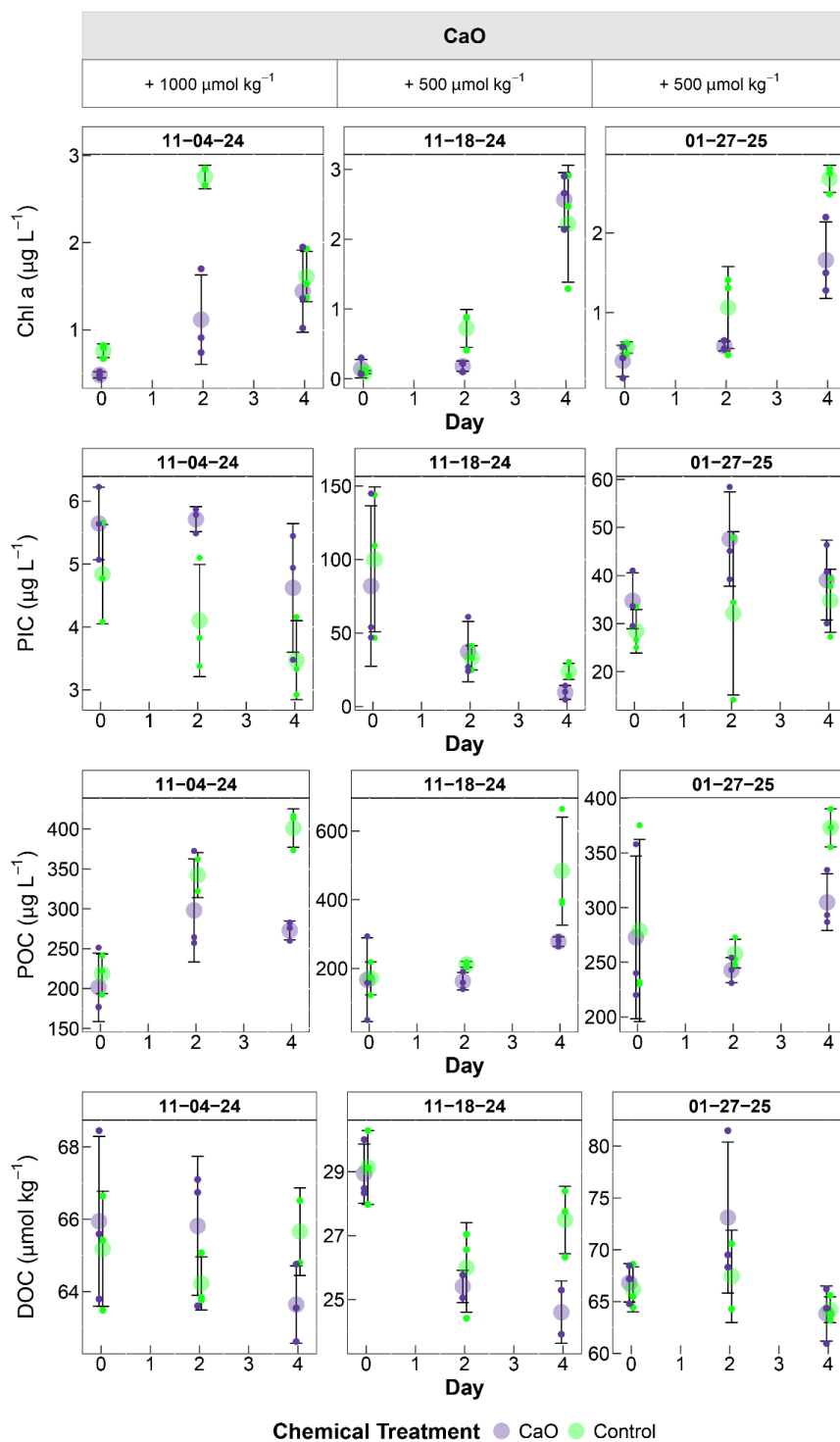
369 We replicated the previous experiment with the goal to capture a lower ambient PIC  
370 signal, but in this experiment the average starting PIC was 6-10 times the normal background  
371 (30-50 μgC L<sup>-1</sup> compared to ~5 μgC L<sup>-1</sup>). Upon CaO addition the system experienced a pH  
372 increase of 0.95 units (pH<sub>f</sub> = 8.63 ± 0.01), and Ω<sub>aragonite</sub> increased from 1.23 ± 0.14 to 8.63 ± 0.16.  
373 While there were samples in which the values of PIC concentration in the treatment samples  
374 averaged higher than the Controls, the overall 4-day trends are not statistically significant  
375 ( $p > 0.05$ , ANOVA and Linear Regression methods). The Control averages 1 μg L<sup>-1</sup> Chl a higher  
376 than the treatment and almost 100 μgC L<sup>-1</sup> POC higher than the treatment by Day 4. Yet, due to  
377 high variability between bottles, the differences in POC and DOC between the controls and  
378 treatment are not statistically different when tested with nonparametric ANOVA or linear  
379 analysis. Of note, the differences in Chl a overtime are statistically significant when analyzed  
380 with a linear regression analysis and a more lenient threshold for significance (Table 4,  $p = 0.08$ ,  
381  $\alpha = 0.1$ ) but are not significant with a nonparametric ANOVA.

382





384 **Figure 4. Summary of Water Chemistry from (CaO) Amendment Experiments.** Panels are grouped  
385 by the alkalinity treatment they received: Controls (green) and CaO (purple). The start date of the  
386 experiment is listed for reference to differentiate between duplicate experiments. The four variables  
387 displayed here are measured Alkalinity ( $\mu\text{mol kg}^{-1}$ ), measured Dissolved Inorganic Carbon (DIC) ( $\mu\text{mol}$   
388  $\text{kg}^{-1}$ ), pH calculated from CO2Sys.v3, and dissolved oxygen ( $\mu\text{mol kg}^{-1}$ ). Each plot shows the average of  
389 the treatment per timepoint ( $n = 3$ ), and the error bars are the standard deviation between the triplicate  
390 bottles. Smaller symbols show individual bottles. As mentioned in the methods section, DIC is  
391 immediately lowered on Day 0 due to an expected dilution by the addition of the CaO stock.





393 **Figure 5. Four Day Timeseries of Biogeochemical Response to Different Alkalinity Enhancements.**

394 Smaller symbols show individual bottles, large symbol shows mean. Error bars are the standard deviation  
 395 between replicates (n = 3). The start date of the experiment and the amount of alkalinity added are  
 396 included as headers for reference. The variables displayed are Chl-a ( $\mu\text{g L}^{-1}$ ), PIC - Particulate Inorganic  
 397 Carbon ( $\mu\text{g L}^{-1}$ ), POC- Particulate Organic Carbon ( $\mu\text{g L}^{-1}$ ), and DOC- Dissolved Organic Carbon ( $\mu\text{mol}$   
 398  $\text{kg}^{-1}$ ).

399 **Table 4. Summary of Linear Model Analysis by Experiment.**

	Experiment Number	[ALK Added]	Variable	Control Slope $\pm$ se	Treatment Slope $\pm$ se	<i>P</i> -value Interaction Term	Significance
06-17-24	NaOH	500	PIC	0.23 $\pm$ 0.17	-0.02 $\pm$ 0.17	0.33	FALSE
	NaOH	500	POC	64.6 $\pm$ 14.5	69.3 $\pm$ 16.1	0.83	FALSE
	NaOH	500	CHL	0.87 $\pm$ 0.29	0.67 $\pm$ 0.33	0.67	FALSE
	NaOH	500	O <sub>2</sub>	4.14 $\pm$ 2.97	4.96 $\pm$ 3.65	0.86	FALSE
07-22-24	NaOH	500	PIC	0.69 $\pm$ 0.17	0.53 $\pm$ 0.17	0.50	FALSE
	NaOH	500	POC	21.4 $\pm$ 7.25	7.03 $\pm$ 7.25	0.18	FALSE
	NaOH	500	DOC	-0.16 $\pm$ 4.63	9.72 $\pm$ 4.63	0.15	FALSE
	NaOH	500	CHL	0.03 $\pm$ 0.12	-0.10 $\pm$ 0.12	0.46	FALSE
	NaOH	500	O <sub>2</sub>	9.61 $\pm$ 1.65	10.5 $\pm$ 1.65	0.69	FALSE
06-24-24	Ca+HCO <sub>3</sub>	500	PIC	-0.16 $\pm$ 0.19	0.02 $\pm$ 0.19	0.53	FALSE
	Ca+ HCO <sub>3</sub>	500	POC	156 $\pm$ 25	170 $\pm$ 28.6	0.73	FALSE
	Ca+ HCO <sub>3</sub>	500	CHL	1.10 $\pm$ 0.54	0.26 $\pm$ 0.54	0.29	FALSE
	Ca+ HCO <sub>3</sub>	500	O <sub>2</sub>	13.5 $\pm$ 2.82	13.1 $\pm$ 3.12	0.93	FALSE
07-15-24	Ca+ HCO <sub>3</sub>	500	PIC	0.72 $\pm$ 0.22	0.68 $\pm$ 0.22	0.91	FALSE
	Ca+ HCO <sub>3</sub>	500	POC	98.4 $\pm$ 16	98.9 $\pm$ 16	0.98	FALSE
	Ca+ HCO <sub>3</sub>	500	DOC	2.83 $\pm$ 5.18	7.05 $\pm$ 5.18	0.57	FALSE
	Ca+ HCO <sub>3</sub>	500	CHL	0.78 $\pm$ 0.47	0.53 $\pm$ 0.47	0.71	FALSE
	Ca+ HCO <sub>3</sub>	500	O <sub>2</sub>	29.3 $\pm$ 2.81	22.8 $\pm$ 3.12	0.14	FALSE
11-18-24	CaO	500	PIC	-19.0 $\pm$ 6.39	-18.1 $\pm$ 6.39	0.92	FALSE
	CaO	500	POC	52.7 $\pm$ 14.4	27.8 $\pm$ 12.9	0.22	FALSE
	CaO	500	DOC	-0.41 $\pm$ 2.9	-1.12 $\pm$ 0.32	0.13	FALSE
	CaO	500	CHL	0.53 $\pm$ 0.12	0.61 $\pm$ 0.21	0.68	FALSE
	CaO	500	O <sub>2</sub>	1.92 $\pm$ 4.13	-0.64 $\pm$ 4.14	0.86	FALSE
01-27-25	CaO	500	PIC	1.58 $\pm$ 1.99	1.08 $\pm$ 1.99	0.86	FALSE
	CaO	500	POC	23.5 $\pm$ 11.1	8.03 $\pm$ 11.1	0.34	FALSE
	CaO	500	DOC	-0.49 $\pm$ 0.53	-0.74 $\pm$ 0.53	0.74	FALSE
	CaO	500	CHL	0.53 $\pm$ 0.08	0.32 $\pm$ 0.08	0.08*	FALSE
	CaO	500	O <sub>2</sub>	13.8 $\pm$ 0.97	10.9 $\pm$ 1.07	NA	<i>n</i> < 3
11-04-24	CaO	1000	PIC	-0.34 $\pm$ 0.15	-0.26 $\pm$ 0.15	0.68	FALSE
	CaO	1000	POC	45.7 $\pm$ 8.85	17.8 $\pm$ 8.85	<b>0.04</b>	<b>TRUE</b>
	CaO	1000	DOC	0.07 $\pm$ 0.36	-0.58 $\pm$ 0.32	0.20	FALSE
	CaO	1000	CHL	0.21 $\pm$ 0.13	0.24 $\pm$ 0.13	0.88	FALSE
	CaO	1000	O <sub>2</sub>	17.2 $\pm$ 4.86	-0.86 $\pm$ 4.37	<b>0.01</b>	<b>TRUE</b>

400 Table shows the slope  $\pm$  the standard error around the slope of the Control and Treatment groups by the  
 401 variable being analyzed. The p-value is shown, and the test result indicating statistical significance is



402 shown when  $p < 0.05$ . The \* marks a relaxed significance threshold ( $\alpha = 0.1$ ). TRUE OR FALSE  
 403 indicates whether the interaction is statistically significant or not. Bold for emphasis. NA written where  
 404 there are less than three data points per time point for control and treatment.

405

406 **Table 5. Summary of Two-Way Non-parametric Analysis of Variance (ANOVA) by**  
 407 **Experiment.**

	Experiment Number	[ALK Added]	Variable	<i>P-value</i> Interaction Term	Significance
06-17-24	NaOH	500	PIC	0.55	FALSE
	NaOH	500	POC	0.88	FALSE
	NaOH	500	CHL	0.88	FALSE
	NaOH	500	O <sub>2</sub>	0.93	FALSE
07-22-24	NaOH	500	PIC	0.52	FALSE
	NaOH	500	POC	0.22	FALSE
	NaOH	500	DOC	0.24	FALSE
	NaOH	500	CHL	0.44	FALSE
	NaOH	500	O <sub>2</sub>	0.86	FALSE
06-24-24	Ca+HCO <sub>3</sub>	500	PIC	0.39	FALSE
	Ca+ HCO <sub>3</sub>	500	POC	0.94	FALSE
	Ca+ HCO <sub>3</sub>	500	CHL	0.56	FALSE
	Ca+ HCO <sub>3</sub>	500	O <sub>2</sub>	0.95	FALSE
07-15-24	Ca+ HCO <sub>3</sub>	500	PIC	0.89	FALSE
	Ca+ HCO <sub>3</sub>	500	POC	0.53	FALSE
	Ca+ HCO <sub>3</sub>	500	DOC	0.18	FALSE
	Ca+ HCO <sub>3</sub>	500	CHL	0.82	FALSE
	Ca+ HCO <sub>3</sub>	500	O <sub>2</sub>	0.83	FALSE
11-18-24	CaO	500	PIC	0.74	FALSE
	CaO	500	POC	0.66	FALSE
	CaO	500	DOC	0.55	FALSE
	CaO	500	CHL	0.71	FALSE
	CaO	500	O <sub>2</sub>	0.98	FALSE
01-27-25	CaO	500	PIC	0.90	FALSE
	CaO	500	POC	0.86	FALSE
	CaO	500	DOC	0.78	FALSE
	CaO	500	CHL	0.97	FALSE
	CaO	500	O <sub>2</sub>	0.74	FALSE
11-04-24	CaO	1000	PIC	0.72	FALSE
	CaO	1000	POC	0.64	FALSE
	CaO	1000	DOC	0.15	FALSE
	CaO	1000	CHL	0.54	FALSE
	CaO	1000	O <sub>2</sub>	0.34	FALSE

408 The Scheirer Ray Hare test is used for this analysis. The interaction between treatment (Control vs.  
 409 Treatment) condition and time on PIC, POC, Chl a, DOC, and dissolved O<sub>2</sub> is summarized by the p-value.



410 TRUE indicates whether the interaction is statistically significant with an ( $\alpha = 0.05$ ), FALSE shows an  
411 insignificant impact on the measured “Variable” column.

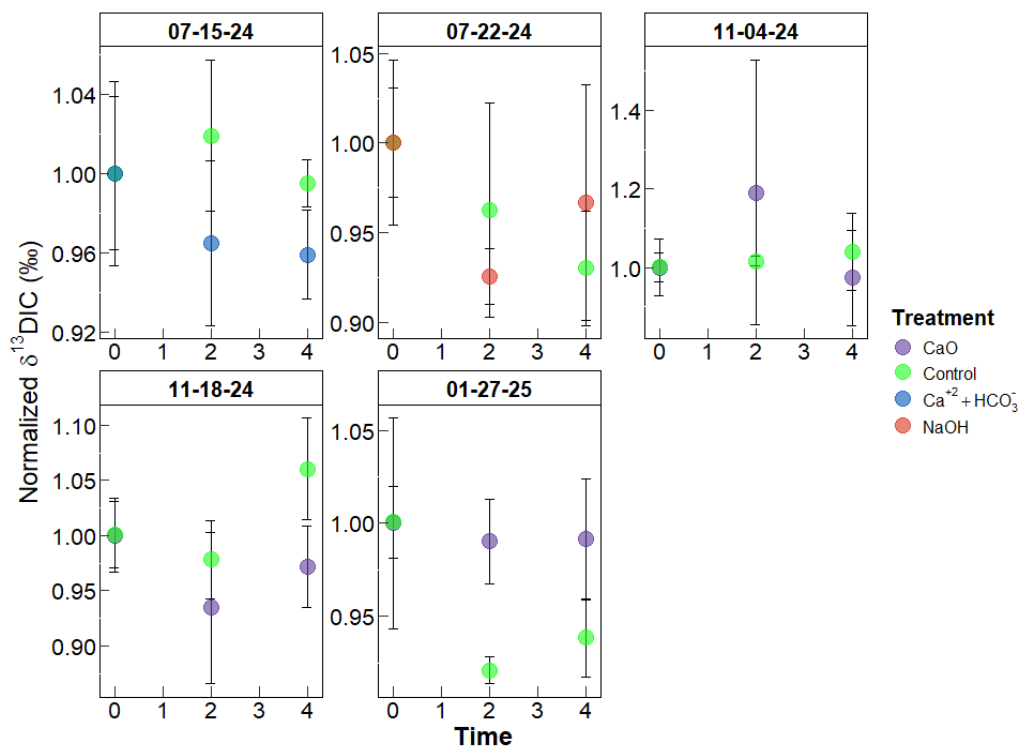
412

### 413 3.4 Carbon Budgets

#### 414 3.4.1 Carbon Isotopes to track Respiration

415 Organic carbon is subject to net increases due to production and decreases attributed to  
416 respiration. We added a  $^{13}\text{C}$  isotope spike to controls and treatment bottles to assess if an  
417 alkalinity addition would change the rate of organic matter remineralization and therefore change  
418 the isotopic signature of the residual seawater. The isotope addition only increased DIC by 2  
419  $\mu\text{mol kg}^{-1}$ , but as this was a separate added stock the starting isotopic  $\delta^{13}\text{DIC}$  varied by bottle.  
420 Hence to compare across various days and treatments, we divided the measured  $\delta^{13}\text{DIC}$  value  
421 from each bottle by the average  $\delta^{13}\text{DIC}$  on Day 0 Control or Treatment value. An increase in  
422 organic matter remineralization would make the pool of  $\delta^{13}\text{DIC}$  lighter. The effect of treatment  
423 on  $\delta^{13}\text{DIC}$  was tested with a two-factor ANOVA where the variables ‘Experiment Day’ and  
424 ‘Treatment’ were taken as factors. The interaction of these factors results in a  $p > 0.05$  for all  
425 experiments. Hence, there were no consistent and sustained changes in the  $\delta^{13}\text{DIC}$  pool of the  
426 treatment bottles when compared to the control bottles (seawater isotopes shown in Fig. 6).  
427 There was also no decrease in the  $\delta^{13}\text{DIC}$  values due to invasion of  $\text{CO}_2$  even in the base  
428 addition experiments, because there was no headspace in the bottles, i.e. this isotope tracer  
429 demonstrated that a closed system was maintained.

430



431

432 **Figure 6. Normalized Seawater (DIC)  $\delta^{13}\text{C}$  ‰ over Time in all Experiments.** Panel (07-15-24) + 500  
 433  $\mu\text{mol kg}^{-1}$   $\text{CaCl}_2$  &  $\text{NaHCO}_3$ , (07-22-24) + 500  $\mu\text{mol kg}^{-1}$   $\text{NaOH}$ , (11-04-24) + 1000  $\mu\text{mol kg}^{-1}$   $\text{CaO}$ , (11-  
 434 18-24) + 500  $\mu\text{mol kg}^{-1}$   $\text{CaO}$  with higher ambient PIC, and (01-27-25) + 500  $\mu\text{mol kg}^{-1}$   $\text{CaO}$ . Each data  
 435 point has an  $n = 3$ , and error bars are the standard deviation of the averaged values. Data was ‘normalized’  
 436 by dividing each measured value with the initial starting  $\delta^{13}\text{C}$  value of the DIC after all bottles were given  
 437 the isotope spike on Day 0.

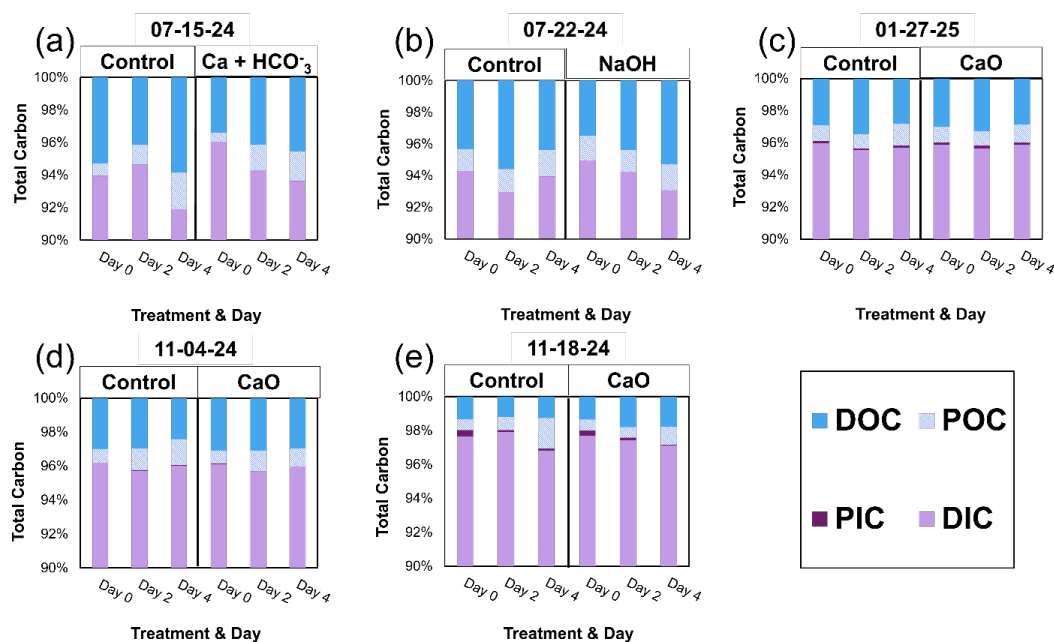
438

### 439 3.4.2 Carbon Partitioning

440 The purpose of conducting closed system experiments was to better understand and  
 441 constrain the partitioning of carbon between various pools after increasing the amount of carbon  
 442 in the dissolved inorganic phase and/or by adjusting alkalinity with a strong base. Here we  
 443 present the distribution of carbon in various pools (DIC, DOC, PIC, POC) and track the  
 444 movement of carbon over the span of four days (Fig. 7). These distributions are generated from  
 445 the mean measured values of triplicate bottles at each time point. In general, ~95 % of the carbon



446 exists as DIC, ~3.5 % is stored as DOC, ~ 1.2 % is found in the POC pool, and < 0.1 % in the  
 447 PIC pool. The non-DIC pool is highly variable across the “Day 0” starting conditions of all  
 448 experiments (summarized in Table 3). The addition of alkalinity does not change carbon  
 449 distribution in most of these experiments (Fig. 7). The decrease in DIC (Panel a & b, Fig. 7) is  
 450 matched by an increase of either POC or DOC. The measured DOC values do not show any  
 451 statistical differences between the treatment and control conditions.



452

453 **Figure 7. Total Carbon Budget for All Experiments.** Panel (a) + 500  $\mu\text{mol kg}^{-1}$   $\text{CaCl}_2$  &  $\text{NaHCO}_3$ , (b) +  
 454 500  $\mu\text{mol kg}^{-1}$   $\text{NaOH}$ , (c) + 500  $\mu\text{mol kg}^{-1}$   $\text{CaO}$ , (d) + 1000  $\mu\text{mol kg}^{-1}$   $\text{CaO}$ , and (e) + 500  $\mu\text{mol kg}^{-1}$   $\text{CaO}$   
 455 with higher (ambient) particles of inorganic carbon. Bar plots are an average of 3 bottles per timepoint.  
 456 Plots show changes in distribution of carbon over the duration of the experiment between treatments and  
 457 controls.

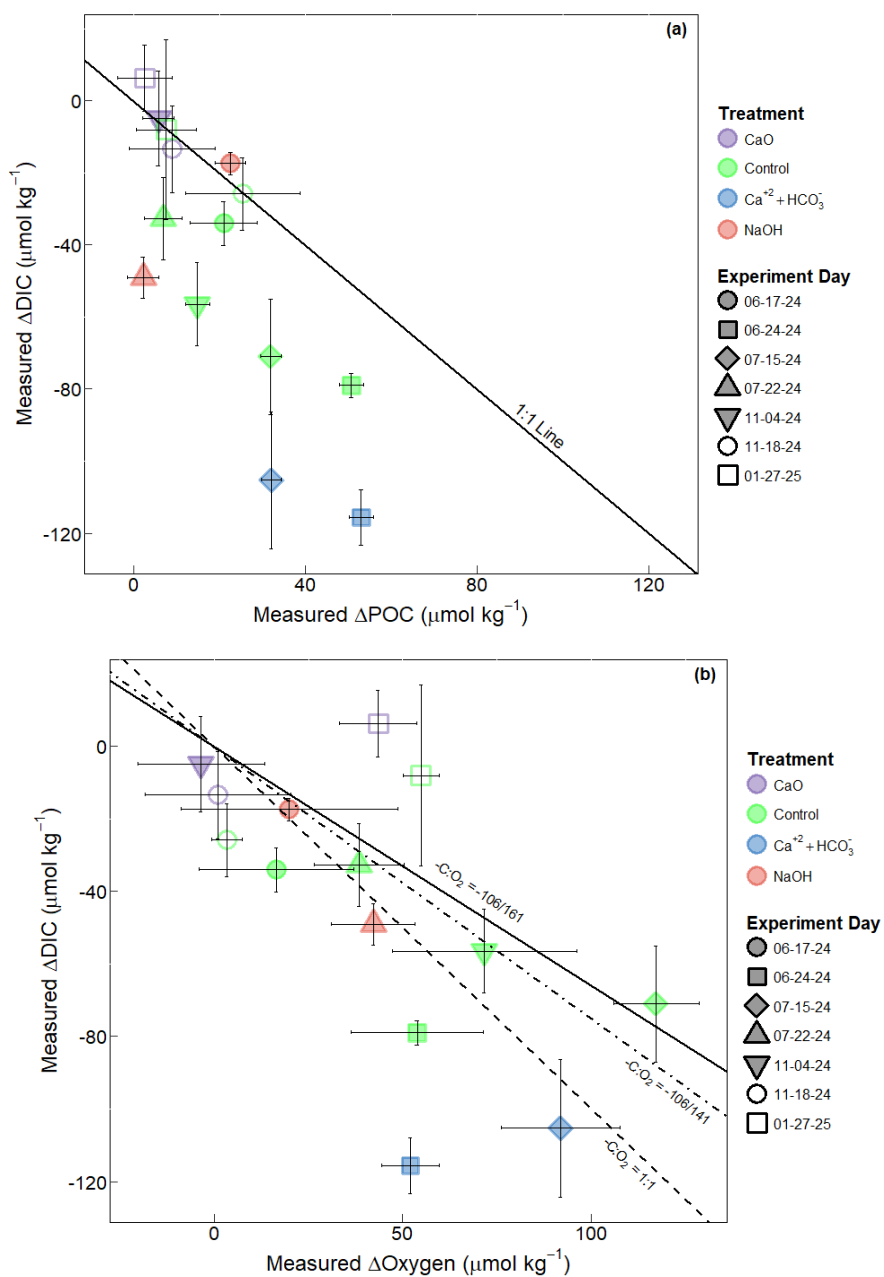
458

459 We compared the total measured DIC decrease with the amount of POC increase over 4  
 460 days to check if our measured carbon pools are stoichiometrically consistent with one another  
 461 and also to see how DOC production may account for some of the DIC drawdown. The  $\text{Ca}^{+2}$  +  
 462  $\text{HCO}_3^-$  treatments fall furthest from a 1:1 relationship (Fig. 8 (a)), which means these



463 experiments show a deficit of POC production relative to DIC drawdown. DIC lost to the  
464 precipitation of calcium carbonate is  $< 1 \mu\text{mol kg}^{-1}$  over 4 days, and  $\text{CO}_2$  lost from the minimal  
465 permeability of the PETG bottles could be at most  $3 \mu\text{mol kg}^{-1} \text{ day}^{-1}$  (assuming  $\text{CO}_2$  permeability  
466 for PETG is  $125 \text{ cc-mil inch}^{-2} \text{ day}^{-1}$ , wall thickness =  $0.76 \text{ mm}$ , surface area  $\sim 300 \text{ inch}^2$  and the  
467  $\Delta p\text{CO}_2$  gradient between water inside the bottle vs. outside in the ocean =  $300 \mu\text{atm}$ ). Figure 8  
468 (a) shows that the  $50\text{-}100 \mu\text{mol kg}^{-1}$  decrease in DIC must lead to greater production of DOC.

469 As an additional test of carbon partitioning, we can check to see whether these  
470 experiments fall within Redfield stoichiometries by comparing the total drawdown of DIC with  
471 the change in dissolved oxygen (Fig. 8 (b)). A range of DIC:O<sub>2</sub> ratios is considered. The calcium  
472 + bicarbonate experiments and one of their controls fall furthest from the range of Redfield  
473 ratios. The same  $\text{Ca}^{+2} + \text{HCO}_3^-$  experiments that show a deficit in POC also show a deficit in  
474 dissolved oxygen than what would be expected if DIC consumption were producing DOC.



475

476

477 **Figure 8. Comparison of Stoichiometric Changes in DIC, Dissolved O<sub>2</sub>, and POC in terms of the**  
 478 **Redfield Ratio.** (a) Cross plot of measured decrease of DIC versus the measured increase of POC; solid  
 479 line is the 1:1 line. Points that fall below the 1:1 line are thought to have increased DOC. (b) Cross plot of  
 480 measured decrease of DIC versus measured production of dissolved oxygen. Plotted lines show the slopes  
 481 of various Redfield Ratios: solid line ( $-C:O_2 = -106/161$ ), dot-dash line ( $-C:O_2 = -106/141$ ), and dashed



482 line ( $-C:O_2 = -106:-106$  i.e. a 1:1 ratio). Ratios taken from (Anderson, 1995). All points in (a) and (b)  
483 have a  $n = 3$ , and the delta is calculated as the difference between the average of Day 0 and Day 4 bottle  
484 values. Error bars are propagated standard deviations of averaged values used to generate the delta values.

485

#### 486 **4. Discussion—Relevance to OAE**

487 If alkalinity is added to the ocean, we would need to know the effects of different  
488 minerals/alkalinity sources – i.e., to test if one is more harmful than another. Thus, we conducted  
489 standardized experiments that raised alkalinity by the same threshold ( $+500 \mu\text{mol kg}^{-1}$ ). The  
490 properties of each alkalinity source (NaOH, CaO, and simulated dissolved limestone -  $\text{NaHCO}_3$   
491 +  $\text{CaCl}_2$ ) created dissimilar carbonate chemistry regimes in the experiments. Here we discuss  
492 how these different regimes influenced abiotic side effects – such as precipitation of minerals  
493 and biotic side effects such as organic matter cycling.

#### 494 **4.1 Secondary Precipitation of $\text{CaCO}_3$**

495 The base addition method for OAE functions on the principle of raising pH which will  
496 promote uptake of atmospheric  $\text{CO}_2$ . Adding dissolved limestone does not drastically raise pH  
497 like NaOH or CaO addition. CaO addition increases both pH and the  $[\text{Ca}^{+2}]$ , hence the resultant  
498 change in  $\Omega_{\text{aragonite}}$  is higher than the change in  $\Omega_{\text{aragonite}}$  after NaOH addition. Yet, even with  
499  $\Omega_{\text{aragonite}} \sim 14$  ( $\text{CaO} + 1000 \mu\text{mol kg}^{-1}$ ) – which is above the threshold for pseudo-homogenous  
500 precipitation in seawater according to Morse and He ( $T = 25 \text{ }^\circ\text{C}$  (Morse and He, 1993)) we do  
501 not see any statistically significant secondary precipitation in these experiments.

502 Our results are consistent with other studies conducting similar manipulations to find the  
503 minimum thresholds of secondary precipitation of  $\text{CaCO}_3$ .  $\text{NaHCO}_3 + \text{Na}_2\text{CO}_3$  additions, below  
504  $\Omega_{\text{aragonite}} < 15$  without  $\text{Ca}^{+2}$  increase, resulted in no precipitation in seawater in the absence of  
505 particles ( $0.2 \mu\text{m}$  filtered) or with small particles ( $55 \mu\text{m}$  filtered) (Hartmann et al., 2023; Moras  
506 et al., 2022; Suitner et al., 2024). In the case of NaOH addition experiments, immediate brucite  
507 ( $\text{Mg}(\text{OH})_2$ ) precipitation was observed in multiple studies (Bach et al., 2024; Ferderer et al.,  
508 2022; Hashim et al., 2025; Ringham et al., 2024; Suitner et al., 2024), but has been shown to  
509 quickly redissolve. ‘Runaway’  $\text{CaCO}_3$  has been observed immediately after NaOH addition at  
510  $\Omega_{\text{aragonite}} > 25$  ( $T = 11\text{-}20 \text{ }^\circ\text{C}$  (Ringham et al., 2024; Suitner et al., 2024) or after 24 hours at  
511  $\Omega_{\text{aragonite}} > 15$  ( $T = 11\text{-}23 \text{ }^\circ\text{C}$ , (Hartmann et al., 2023; Suitner et al., 2024)). Hashim et al. (2025)



512 find  $\text{CaCO}_3$  production after a  $+500 \mu\text{mol kg}^{-1}$  TA enhancement, but their resultant  $\Omega_{\text{aragonite}} = 11$ .  
513 In the range that is comparable to our study ( $\Omega_{\text{aragonite}} = 7.63$  with NaOH), no  $\text{CaCO}_3$  formation  
514 was observed for up to 20 days (Hartmann et al., 2023; Ringham et al., 2024; Suitner et al.,  
515 2024).

516 We expected to see increased PIC formation with the CaO addition experiments ( $\Omega_{\text{aragonite}}$   
517 = 8.5, 8.6, 13.7) because Moras et al., (2022) observed  $\text{CaCO}_3$  precipitation after hydrated lime  
518 addition around  $\Omega_{\text{aragonite}} = 7$ , but their experimental conditions allowed for heterogeneous  
519 precipitation (precipitation on mineral phases), whereas our experimental set-up would have  
520 primarily allowed for pseudo-homogenous precipitation (precipitation on colloids or organic  
521 materials) and it seems that this threshold must be higher than  $\Omega_{\text{aragonite}} = 14$  when using an  
522 aqueous medium to increase alkalinity.

523 Thus far it is clear that the thresholds for heterogeneous precipitation (i.e., relevant if  
524 using mineral feedstock) versus pseudo-homogeneous precipitation (i.e., relevant if primarily  
525 using aqueous solutions for OAE in natural seawater) must be different, and may vary with  
526 different temperature, salinity, or even organic matter content (Berner, 1975; Marion et al., 2009;  
527 Moras et al., 2024; Morse et al., 2007; Morse and He, 1993; Mucci and Morse, 1983; Naviaux et  
528 al., 2019; Nguyen Dang et al., 2017). When considering a broader impact, increasing alkalinity  
529 with NaOH, CaO or even  $\text{CaCl}_2 + \text{NaHCO}_3$  at  $500\text{-}1000 \mu\text{mol kg}^{-1}$  did not significantly increase  
530  $\text{CaCO}_3$  production in waters from LA Harbor with very different ambient PIC concentrations.

## 531 **4.2 Impact of Alkalinity on Organic Matter Cycling**

### 532 **4.2.1 Neutral Impacts of NaOH and Dissolved Limestone Addition**

533 The Port of Los Angeles has a dynamic seasonal cycle that directly influences the carbon  
534 standing stock – driven by the seasonally dominant organisms within the water. The organic C  
535 biomass is highest in Spring at  $300 \mu\text{gC L}^{-1}$ , followed by  $150 \mu\text{gC L}^{-1}$  in Summer,  $100 \mu\text{gC L}^{-1}$  in  
536 Fall, and  $80 \mu\text{gC L}^{-1}$  in the Winter (Connell et al., 2017). There is also seasonality in the types of  
537 organisms that are creating biomass and are thus responding to the alkalinity addition during our  
538 experiments. The NaOH (starting  $[\text{POC}] = 200 \mu\text{gC L}^{-1}$ ) and dissolved Limestone (starting  
539  $[\text{POC}] = 400 \mu\text{gC L}^{-1}$ ) experiments were conducted in the Summer, when Diatoms make up more  
540 than half of the particulate biomass, followed by Picoeukaryotes in the LA Port region (Connell



541 et al., 2017). The lack of a negative impact on primary production after NaOH and dissolved  
542 limestone addition ( $\text{pH} < 8.55$ ) in this study is congruent with results seen from other Diatom  
543 specific studies (Gately et al., 2023; Oberlander et al., 2025) and natural community studies (Guo  
544 et al., 2025) where the resultant change in POC production was also negligible. Other studies  
545 have seen a decrease in Diatom concentration once the alkalinity addition has increased pH  
546 beyond 8.55 (Kousoulas et al., 2025; Oberlander et al., 2025) and note a decrease in  
547 Picoeukaryote concentration after NaOH addition (Federer et al., 2022; Kousoulas et al., 2025;  
548 Oberlander et al., 2025). In this study, we do not have evidence to say if the species compositions  
549 shifted, however, these alkalinity additions did not statistically alter the POC concentrations  
550 when compared to the control (Fig. 3). Federer et al. (2022) saw POC decline after alkalinity  
551 addition, they attributed this to a possible alteration in the composition of the diatom community  
552 and increased heterotrophic bacterial activity in their alkalinity (NaOH and  $\text{NaHCO}_3$ ) treatments.  
553 We also do not see substantial evidence from direct measurements to suggest that calcium and  
554 bicarbonate addition increases the production of DOC above the control samples, however, there  
555 appear to be times in the water mass sampled when DOC production is more prevalent.

556 Of note is the natural variability of pH in LA Harbor waters which has been previously  
557 measured within range 7.57-8.46 (Lyons and Birosik, 2007). Under the conditions of our  
558 incubations, the natural microbial populations may be acclimated to pH shifts of the order  
559 generated by NaOH or  $\text{HCO}_3$  in these experiments ( $\text{pH}$  in Treatments  $< 8.55$ ). Our results  
560 suggest that NaOH addition could change PIC and DOC production in waters incubated in the  
561 dark to simulate decoupling from the euphotic zone (See Supplemental Information), but we  
562 encourage further experiments for more conclusive results.

563

#### 564 **4.2.2 Potential Impact of CaO Addition**

565 The impacts to Chl a and POC from the CaO addition when compared to the unamended  
566 conditions are inconsistent across the experiments conducted in this study. One experiment had a  
567 statistically significant impact to Chl a, which occurs at  $+ 500 \mu\text{mol kg}^{-1}$  but not  $+ 1000 \mu\text{mol kg}^{-1}$ ,  
568 indicating that this result did not reproduce. POC production is reduced by  $100 \mu\text{gC L}^{-1}$  after  
569 4-days from the  $+ 500 \mu\text{mol kg}^{-1}$  CaO additions (but the trend is not statistically significant due  
570 to high initial variability). POC production is reduced by  $200 \mu\text{gC L}^{-1}$  after the  $1000 \mu\text{mol kg}^{-1}$



571 addition, *which is statistically significant*. This coincides with statistically lower dissolved  
572 oxygen after a 1000  $\mu\text{mol kg}^{-1}$  CaO addition. The impacts of CaO addition at +500  $\mu\text{mol kg}^{-1}$   
573 may not be statistically significant on LA Harbor organic matter cycling, but at + 1000  $\mu\text{mol kg}^{-1}$   
574 these results do become statistically significant.

575 Other studies that test the impact of ocean liming – either simulated by CaO,  $\text{Ca}(\text{OH})_2$ , or  
576 even NaOH +  $\text{CaCl}_2$  addition – have seen minimal effects on growth rates, grazing rate, and  
577 community composition when the resultant change has been below pH 9 (de Castro et al., 2025;  
578 Traboni et al., 2025). In our study the starting pH of the seawater is around 7.68-7.85 and the  
579 CaO additions bring this pH to 8.57-8.91. When the CaO addition raises pH above 9, a couple of  
580 studies have shown a decrease in organism quality (i.e., nutrient composition) and growth rate  
581 (Bhaumik et al., 2025) or decreased motility and even increased mortality depending on the  
582 exposure time to elevated pH (Camatti et al., 2024; Pedersen and Hansen, 2003). CaO addition,  
583 that reduces  $\text{pCO}_2$  below  $\sim 100 \mu\text{atm}$  (in our study this is observed only during CaO + 1000  
584  $\mu\text{mol kg}^{-1}$ ), could cause issues in primary production from the  $\text{CO}_2$  limitation. This has been  
585 shown in coccolithophore performance (Bach et al., 2011; Faucher et al., 2025; Riebesell et al.,  
586 1993; Sett et al., 2014) and some other marine phytoplankton (Hansen, 2002; Pedersen and  
587 Hansen, 2003). These results draw attention to how reorganization of community composition  
588 (with smaller phytoplankton that are better adapted to lower  $\text{pCO}_2$  availability (Chrachri et al.,  
589 2018; Flynn et al., 2012; Wolf-Gladrow and Riebesell, 1997)) could reduce the transfer  
590 efficiency of POM to the deeper ocean (Boyd and Newton, 1995). In this study we do not  
591 incorporate a characterization of size classes, but future alkalinity enhancement studies should  
592 also try to incorporate an analysis of changes in particle size class, among a suite of other  
593 ecological impacts (Marx et al., 2025 Preprint).

594

## 595 **5. Conclusions**

596 When considering the impacts of various minerals used to simulate OAE on carbon  
597 partitioning in a natural marine plankton community, we see no overall trends that could be  
598 statistically significant suggesting secondary precipitation of  $\text{CaCO}_3$ . Our experiments show that  
599 even factors that should increase the likelihood of  $\text{CaCO}_3$  precipitation – supersaturation &  
600 greater nucleation sites – will not always result in precipitation. In the case of LA Harbor waters,



601 there may be microbial communities that are not sensitive nor responsive to the amount of  
602 alkalinity added in these experiments. There also may be other environmental parameters that  
603 influence POC and PIC production more than alkalinity enhancement. Conducting more  
604 experiments across a wide range of waters and ecosystems is recommended.

605 Chl a did not always reliably track organic matter production and should not be used as a  
606 proxy for POC. In our waters, sometimes POC increased and sometimes it decreased over 4-day  
607 incubations. However, there was a consistent pattern of less POC production in CaO added  
608 treatment bottles—lower by 100-200  $\mu\text{gC L}^{-1}$  compared to control samples. From our work, CaO  
609 additions are potentially harmful to the production of POC— but we encourage further studies on  
610 changes in particle class size, and studies that may leverage ‘omics tools to understand what  
611 parts of the organic matter cycle may be impacted by CaO addition.

612 We do not see statistically significant changes in production of particulate and dissolved  
613 organic matter after NaOH and Dissolved Limestone alkalinity addition as compared to control  
614 waters (untreated). Future studies should draw attention to the impacts of increased alkalinity in  
615 regions where the amended water mass is lost from the euphotic zone, where primarily  
616 heterotrophic reactions occur. This may require expanding our understanding of downstream  
617 trophic level concerns of OAE.

618

#### 619 *Data Availability*

620 Data are publicly available at [https://github.com/ruchap-wani/Wani-et-al-OAE-Carbon-](https://github.com/ruchap-wani/Wani-et-al-OAE-Carbon-Partitioning)  
621 [Partitioning](https://github.com/ruchap-wani/Wani-et-al-OAE-Carbon-Partitioning)

622

#### 623 *Author Contributions*

624 RW and WB designed the experiments with consultation from NR. RW conducted these  
625 experiments with the help of DR, RA, and EJ. RW was responsible for sample analysis, data  
626 curation, and formal statistical analysis with consultation from NR and WB. Funding was  
627 acquired by WB. The manuscript was written and edited by RW with contributions from WB.

628

#### 629 *Competing Interests*

630 WB is the co-founder of Calcarea, Inc. The authors declare that they have no other competing  
631 interests.



632

633 *Acknowledgements*

634 We would like to thank the USC Wrigley Institute of Environment and Sustainability, AltaSea,  
635 and Calcearia (Pierre Forin), for access to their laboratory and dock resources. We also would like  
636 to thank Doug Capone, Myrna Jacobson, Sarah Feakins, and the Department of Environmental  
637 Engineering at the University of Southern California for access to their instruments to make Chl-  
638 a and dissolved organic carbon measurements.

639

640 *Financial Support*

641 This research was conducted while RW was a recipient of the Wrigley Institute Graduate  
642 Fellowship in 2023. The research was funded by the Lott Innovation Award and the Faculty  
643 Innovation Award (to WB) through the USC Wrigley Institute for Environmental Studies  
644 (WIES). We acknowledge an NSF-REU award to USC WIES for support of RA (2024) and a  
645 Zinsmeyer Summer Research Award to EJM (2023) through grant no. OCE-2244583.

646

647

648

649 **References**

- 650 Anderson, L. A.: On the hydrogen and oxygen content of marine phytoplankton, Deep-Sea  
651 Research Part I, 42, 1675–1680, [https://doi.org/10.1016/0967-0637\(95\)00072-E](https://doi.org/10.1016/0967-0637(95)00072-E), 1995.
- 652 Archer, D. E.: An atlas of the distribution of calcium carbonate in sediments of the deep sea,  
653 Global Biogeochem. Cycles, 10, 159–174, <https://doi.org/10.1029/95GB03016>, 1996.
- 654 Bach, L. T., Riebesell, U., and Schulz, K. G.: Distinguishing between the effects of ocean  
655 acidification and ocean carbonation in the coccolithophore *Emiliana huxleyi*, Limnol.  
656 Oceanogr., 56, 2040–2050, <https://doi.org/10.4319/lo.2011.56.6.2040>, 2011.
- 657 Bach, L. T., Gill, S. J., Rickaby, R. E. M., Gore, S., and Renforth, P.: CO<sub>2</sub> Removal With  
658 Enhanced Weathering and Ocean Alkalinity Enhancement: Potential Risks and Co-benefits for  
659 Marine Pelagic Ecosystems, Frontiers in Climate, 1, <https://doi.org/10.3389/fclim.2019.00007>,  
660 2019.
- 661 Bach, L. T., Ferderer, A. J., LaRoche, J., and Schulz, K. G.: Technical note: Ocean Alkalinity  
662 Enhancement Pelagic Impact Intercomparison Project (OAEPPIP), Biogeosciences, 21, 3665–  
663 3676, <https://doi.org/10.5194/bg-21-3665-2024>, 2024.
- 664 Barker, S., Archer, D., Booth, L., Elderfield, H., Henderiks, J., and Rickaby, R. E. M.: Globally  
665 increased pelagic carbonate production during the Mid-Brunhes dissolution interval and the CO<sub>2</sub>



- 666 paradox of MIS 11, *Quat. Sci. Rev.*, 25, 3278–3293,  
667 <https://doi.org/10.1016/j.quascirev.2006.07.018>, 2006.
- 668 Berelson, W. M., Balch, W. M., Najjar, R., Feely, R. A., Sabine, C., and Lee, K.: Relating  
669 estimates of CaCO<sub>3</sub> production, export, and dissolution in the water column to measurements of  
670 CaCO<sub>3</sub> rain into sediment traps and dissolution on the sea floor: A revised global carbonate  
671 budget, *Global Biogeochem. Cycles*, 21, 1–15, <https://doi.org/10.1029/2006GB002803>, 2007.
- 672 Berner, R. A.: The role of magnesium in the crystal growth of calcite and aragonite from sea  
673 water, *Geochim. Cosmochim. Acta*, 39, 489–504, [https://doi.org/10.1016/0016-7037\(75\)90102-](https://doi.org/10.1016/0016-7037(75)90102-7)  
674 7, 1975.
- 675 Bhaumik, A., Faucher, G., Henning, M., Meunier, C. L., and Boersma, M.: Prey dynamics as a  
676 buffer: enhancing copepod resilience to ocean alkalinity enhancement, *Environmental Research*  
677 *Letters*, 20, <https://doi.org/10.1088/1748-9326/adaa8c>, 2025.
- 678 Bialonski, S., Caron, D. A., Schloen, J., Feudel, U., Kantz, H., and Moorthi, S. D.: Phytoplankton  
679 dynamics in the Southern California Bight indicate a complex mixture of transport and biology,  
680 *J. Plankton Res.*, 38, 1077–1091, <https://doi.org/10.1093/plankt/fbv122>, 2016.
- 681 Boyd, P. and Newton, P.: Evidence of the potential influence of planktonic community structure  
682 on the interannual variability of particulate organic carbon flux, *Deep Sea Research Part I:*  
683 *Oceanographic Research Papers*, 42, 619–639, [https://doi.org/10.1016/0967-0637\(95\)00017-Z](https://doi.org/10.1016/0967-0637(95)00017-Z),  
684 1995.
- 685 Cai, W.-J. and Jiao, N.: Wastewater alkalinity addition as a novel approach for ocean negative  
686 carbon emissions, *The Innovation*, 3, 100272, <https://doi.org/10.1016/j.xinn.2022.100272>, 2022.
- 687 Camatti, E., Valsecchi, S., Caserini, S., Barbaccia, E., Santinelli, C., Basso, D., and Azzellino, A.:  
688 Short-term impact assessment of ocean liming: A copepod exposure test, *Mar. Pollut. Bull.*, 198,  
689 115833, <https://doi.org/10.1016/j.marpolbul.2023.115833>, 2024.
- 690 Caron, D. A., Connell, P. E., Schaffner, R. A., Schnetzer, A., Fuhrman, J. A., Countway, P. D.,  
691 and Kim, D. Y.: Planktonic food web structure at a coastal time-series site: I. Partitioning of  
692 microbial abundances and carbon biomass, *Deep Sea Research Part I: Oceanographic Research*  
693 *Papers*, 121, 14–29, <https://doi.org/10.1016/j.dsr.2016.12.013>, 2017.
- 694 Carter, C. M., Ross, A. H., Schiel, D. R., Howard-Williams, C., and Hayden, B.: In situ  
695 microcosm experiments on the influence of nitrate and light on phytoplankton community  
696 composition, *J. Exp. Mar. Biol. Ecol.*, 326, 1–13, <https://doi.org/10.1016/j.jembe.2005.05.006>,  
697 2005.
- 698 de Castro, I., Ribeiro, S. C., Louvado, A., Gomes, N. C. M., Cachão, M., Brito de Azevedo, E.,  
699 and Barcelos e Ramos, J.: Ocean liming effect on a North Atlantic microbial community:  
700 changes in composition and rates, *Front. Mar. Sci.*, 12,  
701 <https://doi.org/10.3389/fmars.2025.1602158>, 2025.



- 702 Chrachri, A., Hopkinson, B. M., Flynn, K., Brownlee, C., and Wheeler, G. L.: Dynamic changes  
703 in carbonate chemistry in the microenvironment around single marine phytoplankton cells, *Nat.*  
704 *Commun.*, 9, 74, <https://doi.org/10.1038/s41467-017-02426-y>, 2018.
- 705 Connell, P. E., Campbell, V., Gellene, A. G., Hu, S. K., and Caron, D. A.: Planktonic food web  
706 structure at a coastal time-series site: II. Spatiotemporal variability of microbial trophic activities,  
707 *Deep Sea Research Part I: Oceanographic Research Papers*, 121, 210–223,  
708 <https://doi.org/10.1016/j.dsr.2017.01.007>, 2017.
- 709 Daehler, C. C. and Strong, D. R.: Can You Bottle Nature? The Roles of Microcosms in  
710 *Ecological Research, Ecology*, 77, 663–664, <https://doi.org/10.2307/2265487>, 1996.
- 711 Dickson, A. G.: Thermodynamics of the dissociation of boric acid in synthetic seawater from  
712 273.15 to 318.15 K, *Deep Sea Research Part A. Oceanographic Research Papers*, 37, 755–766,  
713 [https://doi.org/10.1016/0198-0149\(90\)90004-F](https://doi.org/10.1016/0198-0149(90)90004-F), 1990.
- 714 Dickson, A. G. and Millero, F. J.: A comparison of the equilibrium constants for the dissociation  
715 of carbonic acid in seawater media, *Deep Sea Research Part A. Oceanographic Research Papers*,  
716 34, 1733–1743, [https://doi.org/10.1016/0198-0149\(87\)90021-5](https://doi.org/10.1016/0198-0149(87)90021-5), 1987.
- 717 Dong, S., Berelson, W. M., Forin, P., Gutierrez, M., Carroll, D., Menemenlis, D., Kyi, A. Y., and  
718 Adkins, J. F.: Potential of CO<sub>2</sub> sequestration through accelerated weathering of limestone on  
719 ships, *Sci. Adv.*, 11, <https://doi.org/10.1126/sciadv.adr7250>, 2025.
- 720 Dunne, J. P., Sarmiento, J. L., and Gnanadesikan, A.: A synthesis of global particle export from  
721 the surface ocean and cycling through the ocean interior and on the seafloor, *Global*  
722 *Biogeochem. Cycles*, 21, <https://doi.org/10.1029/2006GB002907>, 2007.
- 723 Eisaman, M. D., Geilert, S., Renforth, P., Bastianini, L., Campbell, J., Dale, A. W., Foteinis, S.,  
724 Grasse, P., Hawrot, O., Löscher, C. R., Rau, G. H., and Rønning, J.: Assessing the technical  
725 aspects of ocean-alkalinity-enhancement approaches, *State of the Planet, 2-oae2023*, 1–29,  
726 <https://doi.org/10.5194/sp-2-oae2023-3-2023>, 2023.
- 727 Falkowski, P., Scholes, R. J., Boyle, E., Canadell, J., Canfield, D., Elser, J., Gruber, N., Hibbard,  
728 K., Högberg, P., Linder, S., Mackenzie, F. T., Moore III, B., Pedersen, T., Rosenthal, Y.,  
729 Seitzinger, S., Smetacek, V., and Steffen, W.: The Global Carbon Cycle: A Test of Our  
730 Knowledge of Earth as a System, *Science (1979)*, 290, 291–296,  
731 <https://doi.org/10.1126/science.290.5490.291>, 2000.
- 732 Faucher, G., Haunost, M., Paul, A. J., Tietz, A. U. C., and Riebesell, U.: Growth response of  
733 *Emiliania huxleyi* to ocean alkalinity enhancement, *Biogeosciences*, 22, 405–415,  
734 <https://doi.org/10.5194/bg-22-405-2025>, 2025.
- 735 Ferderer, A., Chase, Z., Kennedy, F., Schulz, K. G., and Bach, L. T.: Assessing the influence of  
736 ocean alkalinity enhancement on a coastal phytoplankton community, *Biogeosciences*, 19, 5375–  
737 5399, <https://doi.org/10.5194/bg-19-5375-2022>, 2022.



- 738 Flynn, K. J., Blackford, J. C., Baird, M. E., Raven, J. A., Clark, D. R., Beardall, J., Brownlee, C.,  
739 Fabian, H., and Wheeler, G. L.: Changes in pH at the exterior surface of plankton with ocean  
740 acidification, *Nat. Clim. Chang.*, 2, 510–513, <https://doi.org/10.1038/nclimate1489>, 2012.
- 741 Fraser, L. H. and Keddy, P.: The role of experimental microcosms in ecological research, *Trends*  
742 *Ecol. Evol.*, 12, 478–481, [https://doi.org/10.1016/S0169-5347\(97\)01220-2](https://doi.org/10.1016/S0169-5347(97)01220-2), 1997.
- 743 Gately, J. A., Kim, S. M., Jin, B., Brzezinski, M. A., and Iglesias-Rodriguez, M. D.:  
744 Coccolithophores and diatoms resilient to ocean alkalinity enhancement: A glimpse of hope?,  
745 *Sci. Adv.*, 9, <https://doi.org/10.1126/sciadv.adg6066>, 2023.
- 746 Giesy, J. P. : Microcosms in ecological research : selected papers from a symposium held at  
747 Augusta, Georgia, November 8-10, 1978, Technical Information Center, U.S. Dept. of Energy ;  
748 Available from National Technical Information Service, U.S. Dept. of Commerce, 1110 pp.,  
749 1980.
- 750 Guo, J. A., Strzepek, R. F., Yuan, Z., Swadling, K. M., Townsend, A. T., Achterberg, E. P.,  
751 Browning, T. J., and Bach, L. T.: Effects of ocean alkalinity enhancement on plankton in the  
752 Equatorial Pacific, *Commun. Earth Environ.*, 6, <https://doi.org/10.1038/s43247-025-02248-7>,  
753 2025.
- 754 Hansen, P.: Effect of high pH on the growth and survival of marine phytoplankton: implications  
755 for species succession, *Aquatic Microbial Ecology*, 28, 279–288,  
756 <https://doi.org/10.3354/ame028279>, 2002.
- 757 Hartmann, J., Suitner, N., Lim, C., Schneider, J., Marín-Samper, L., Aristegui, J., Renforth, P.,  
758 Taucher, J., and Riebesell, U.: Stability of alkalinity in ocean alkalinity enhancement (OAE)  
759 approaches - consequences for durability of CO<sub>2</sub> storage, *Biogeosciences*, 20, 781–802,  
760 <https://doi.org/10.5194/bg-20-781-2023>, 2023.
- 761 Hashim, M. S., Marx, L., Klein, F., Dean, C. L., Burdige, E., Hayden, M., McCorkle, D. C., and  
762 Subhas, A. V.: Mineral formation during shipboard ocean alkalinity enhancement experiments in  
763 the North Atlantic, *Biogeosciences*, 22, 7149–7165, <https://doi.org/10.5194/bg-22-7149-2025>,  
764 2025.
- 765 Iglesias-Rodríguez, M. D., Rickaby, R. E. M., Singh, A., and Gately, J. A.: Laboratory  
766 experiments in ocean alkalinity enhancement research, *State of the Planet*, 2-oae2023, 1–18,  
767 <https://doi.org/10.5194/sp-2-oae2023-5-2023>, 2023.
- 768 Ives, A. R., Foufopoulos, J., Klopfer, E. D., Klug, J. L., and Palmer, T. M.: Bottle or Big-Scale  
769 Studies: How do we do Ecology?, *Ecology*, 77, 681–685, <https://doi.org/10.2307/2265491>, 1996.
- 770 Kheshgi, H. S.: Sequestering atmospheric carbon dioxide by increasing ocean alkalinity, *Energy*,  
771 20, 915–922, [https://doi.org/10.1016/0360-5442\(95\)00035-F](https://doi.org/10.1016/0360-5442(95)00035-F), 1995.
- 772 Kousoulas, K., Ferderer, A., Eriksen, R., and Bach, L. T.: Winners and losers under hydroxide-  
773 based ocean alkalinity enhancement in a Tasmanian plankton community, *J. Phycol.*,  
774 <https://doi.org/10.1111/jpy.70052>, 2025.



- 775 de la Broise, D. and Palenik, B.: Immersed in situ microcosms: A tool for the assessment of  
776 pollution impact on phytoplankton, *J. Exp. Mar. Biol. Ecol.*, 341, 274–281,  
777 <https://doi.org/10.1016/J.JEMBE.2006.10.045>, 2007.
- 778 Lawton, J. H., Naeem, S., Woodfin, R. M., Brown, V. K., Gange, A., Godfray, H. J. C., Heads, P.  
779 A., Lawler, S., Magda, D., Thomas, C. D., Thompson, L. J., and Young, S.: The Ecotron: a  
780 controlled environmental facility for the investigation of population and ecosystem processes,  
781 *Philos. Trans. R. Soc. Lond. B Biol. Sci.*, 341, 181–194, <https://doi.org/10.1098/rstb.1993.0102>,  
782 1993.
- 783 Lee, K., Kim, T.-W., Byrne, R. H., Millero, F. J., Feely, R. A., and Liu, Y.-M.: The universal ratio  
784 of boron to chlorinity for the North Pacific and North Atlantic oceans, *Geochim. Cosmochim.*  
785 *Acta*, 74, 1801–1811, <https://doi.org/10.1016/j.gca.2009.12.027>, 2010.
- 786 Lunstrum, A. and Berelson, W.: CaCO<sub>3</sub> dissolution in carbonate-poor shelf sands increases with  
787 ocean acidification and porewater residence time, *Geochim. Cosmochim. Acta*, 329, 168–184,  
788 <https://doi.org/10.1016/j.gca.2022.04.031>, 2022.
- 789 Lunstrum, A., Keller, D., Hartmann, J., Moras, C., and Wilcox, J.: A framework for  
790 understanding efficiency losses of Ocean Alkalinity Enhancement, in: Goldschmidt 2025  
791 Conference, 2025.
- 792 Lyons, M. J. and Birosik, S.: WATER QUALITY IN THE DOMINGUEZ CHANNEL AND LOS  
793 ANGELES/LONG BEACH HARBOR WATERSHED MANAGEMENT AREA , 2007.
- 794 Marion, G. M., Millero, F. J., and Feistel, R.: Precipitation of solid phase calcium carbonates and  
795 their effect on application of seawater SA-T-P models, *Ocean Science*, 5, 285–291,  
796 <https://doi.org/10.5194/os-5-285-2009>, 2009.
- 797 Marx, L., Rheuban, J., McCorkle, D., Murray, C., Guo, Y., Wang, Z., Michel, A., Chen, K., Kim,  
798 H., and Subhas, A.: Development of the ecological activity index as an integrative ecosystem  
799 assessment and monitoring asset for ocean alkalinity enhancement,  
800 <https://doi.org/10.21203/rs.3.rs-6371725/v1>, 28 May 2025.
- 801 Moras, C. A., Bach, L. T., Cyronak, T., Joannes-Boyau, R., and Schulz, K. G.: Ocean alkalinity  
802 enhancement - avoiding runaway CaCO<sub>3</sub> precipitation during quick and hydrated lime  
803 dissolution, *Biogeosciences*, 19, 3537–3557, <https://doi.org/10.5194/bg-19-3537-2022>, 2022.
- 804 Moras, C. A., Cyronak, T., Bach, L. T., Joannes-Boyau, R., and Schulz, K. G.: Effects of grain  
805 size and seawater salinity on magnesium hydroxide dissolution and secondary calcium carbonate  
806 precipitation kinetics: implications for ocean alkalinity enhancement, *Biogeosciences*, 21, 3463–  
807 3475, <https://doi.org/10.5194/bg-21-3463-2024>, 2024.
- 808 Morse, J. W. and He, S.: Influences of T, S and PCO<sub>2</sub> on the pseudo-homogeneous precipitation  
809 of CaCO<sub>3</sub> from seawater: implications for whiting formation, *Mar. Chem.*, 41, 291–297,  
810 [https://doi.org/10.1016/0304-4203\(93\)90261-L](https://doi.org/10.1016/0304-4203(93)90261-L), 1993.



- 811 Morse, J. W., Arvidson, R. S., and Lüttge, A.: Calcium Carbonate Formation and Dissolution,  
812 Chem. Rev., 107, 342–381, <https://doi.org/10.1021/cr050358j>, 2007.
- 813 Mucci, A. and Morse, J. W.: The incorporation of Mg<sup>2+</sup> and Sr<sup>2+</sup> into calcite overgrowths:  
814 influences of growth rate and solution composition, Geochim. Cosmochim. Acta, 47, 217–233,  
815 [https://doi.org/10.1016/0016-7037\(83\)90135-7](https://doi.org/10.1016/0016-7037(83)90135-7), 1983.
- 816 National Academies of Sciences, E. and M.: A Research Strategy for Ocean-based Carbon  
817 Dioxide Removal and Sequestration, National Academies Press, Washington, DC, 1–308 pp.,  
818 <https://doi.org/10.17226/26278>, 2022.
- 819 Naviaux, J. D., Subhas, A. V., Dong, S., Rollins, N. E., Liu, X., Byrne, R. H., Berelson, W. M.,  
820 and Adkins, J. F.: Calcite dissolution rates in seawater: Lab vs. in-situ measurements and  
821 inhibition by organic matter, Mar. Chem., 215, 103684,  
822 <https://doi.org/10.1016/j.marchem.2019.103684>, 2019.
- 823 Nguyen Dang, D., Gascoïn, S., Zanibellato, A., G. Da Silva, C., Lemoine, M., Riffault, B., Sabot,  
824 R., Jeannin, M., Chateigner, D., and Gil, O.: Role of Brucite Dissolution in Calcium Carbonate  
825 Precipitation from Artificial and Natural Seawaters, Cryst. Growth Des., 17, 1502–1513,  
826 <https://doi.org/10.1021/acs.cgd.6b01305>, 2017.
- 827 Oberlander, J. L., Burke, M. E., London, C. A., and Macintyre, H. L.: Assessing the impacts of  
828 simulated ocean alkalinity enhancement on viability and growth of nearshore species of  
829 phytoplankton, Biogeosciences, 22, 499–512, <https://doi.org/10.5194/bg-22-499-2025>, 2025.
- 830 Paul, A. J., Haunost, M., Goldenberg, S. U., Hartmann, J., Sánchez, N., Schneider, J., Suitner, N.,  
831 and Riebesell, U.: Ocean alkalinity enhancement in an open ocean ecosystem: Biogeochemical  
832 responses and carbon storage durability, EGU sphere, 2024, 1–31,  
833 <https://doi.org/10.5194/egusphere-2024-417>, 2024.
- 834 Pedersen, F. and Hansen, P.: Effects of high pH on a natural marine planktonic community, Mar.  
835 Ecol. Prog. Ser., 260, 19–31, <https://doi.org/10.3354/meps260019>, 2003.
- 836 Perez, F. F. and Fraga, F.: Association constant of fluoride and hydrogen ions in seawater, Mar.  
837 Chem., 21, 161–168, [https://doi.org/10.1016/0304-4203\(87\)90036-3](https://doi.org/10.1016/0304-4203(87)90036-3), 1987.
- 838 Pierrot, D., Epitalon, J. M., Orr, J. C., Lewis, E., and Wallace, D. W. R.: MS Excel program  
839 developed for CO<sub>2</sub> system calculations – version 3.0, 2021.
- 840 Pukelsheim, F.: The Three Sigma Rule, Am. Stat., 48, 88–91,  
841 <https://doi.org/10.1080/00031305.1994.10476030>, 1994.
- 842 Rau, G. H. and Caldeira, K.: Enhanced carbonate dissolution: A means of sequestering waste  
843 CO<sub>2</sub> as ocean bicarbonate, Energy Convers. Manag., 40, 1803–1813,  
844 [https://doi.org/10.1016/S0196-8904\(99\)00071-0](https://doi.org/10.1016/S0196-8904(99)00071-0), 1999.
- 845 Renforth, P.: Perspective: The European Union is not prepared for geochemical carbon dioxide  
846 removal\*, N<sup>o</sup>, 37–72 pp., 2025.



- 847 Renforth, P. and Henderson, G.: Assessing ocean alkalinity for carbon sequestration, *Reviews of*  
848 *Geophysics*, 55, 636–674, <https://doi.org/10.1002/2016RG000533>, 2017.
- 849 Ridgwell, A. and Zeebe, R.: The role of the global carbonate cycle in the regulation and  
850 evolution of the Earth system, *Earth Planet. Sci. Lett.*, 234, 299–315,  
851 <https://doi.org/10.1016/j.epsl.2005.03.006>, 2005.
- 852 Riebesell, U., Wolf-Gladrow, D. A., and Smetacek, V.: Carbon dioxide limitation of marine  
853 phytoplankton growth rates, *Nature*, 361, 249–251, <https://doi.org/10.1038/361249a0>, 1993.
- 854 Riebesell, U., Zondervan, I., Rost, B., Tortell, P. D., Zeebe, R. E., and Morel, F. M. M.: Reduced  
855 calcification of marine plankton in response to increased atmospheric CO<sub>2</sub>, *Nature*, 407, 364–  
856 367, <https://doi.org/10.1038/35030078>, 2000.
- 857 Riebesell, U., Körtzinger, A., and Oschlies, A.: Sensitivities of marine carbon fluxes to ocean  
858 change, *Proceedings of the National Academy of Sciences*, 106, 20602–20609,  
859 <https://doi.org/10.1073/pnas.0813291106>, 2009.
- 860 Riebesell, U., Lee, K., Nejtgaard, J. C., and Fisheries, I.: Pelagic mesocosms Part 2 :  
861 Experimental design of perturbation experiments Pelagic mesocosms, 2010.
- 862 Ringham, M. C., Hirtle, N., Shaw, C., Lu, X., Herndon, J., Carter, B. R., and Eisaman, M. D.: An  
863 assessment of ocean alkalinity enhancement using aqueous hydroxides: kinetics, efficiency, and  
864 precipitation thresholds, *Biogeosciences*, 21, 3551–3570, [https://doi.org/10.5194/bg-21-3551-](https://doi.org/10.5194/bg-21-3551-2024)  
865 2024, 2024.
- 866 Savoie, A. M., Ringham, M., Torres Sanchez, C., Carter, B. R., Dougherty, S., Feely, R. A.,  
867 Hegeman, D., Herndon, J., Khangaonkar, T., Loretz, J., Minck, T., Pelman, T., Premathilake, L.,  
868 Subban, C., Vance, J., and Ward, N. D.: Novel field trial for ocean alkalinity enhancement using  
869 electrochemically derived aqueous alkalinity, *Frontiers in Environmental Engineering*, 4,  
870 <https://doi.org/10.3389/fenv.2025.1641277>, 2025.
- 871 Sett, S., Bach, L. T., Schulz, K. G., Koch-Klavsen, S., Lebrato, M., and Riebesell, U.:  
872 Temperature Modulates Coccolithophorid Sensitivity of Growth, Photosynthesis and  
873 Calcification to Increasing Seawater pCO<sub>2</sub>, *PLoS One*, 9, e88308,  
874 <https://doi.org/10.1371/journal.pone.0088308>, 2014.
- 875 Stachowski-Haberkorn, S., Becker, B., Marie, D., Haberkorn, H., Coroller, L., and de la Broise,  
876 D.: Impact of Roundup on the marine microbial community, as shown by an in situ microcosm  
877 experiment, *Aquatic Toxicology*, 89, 232–241, <https://doi.org/10.1016/j.aquatox.2008.07.004>,  
878 2008.
- 879 Subhas, A. V., Rollins, N. E., Berelson, W. M., Dong, S., Erez, J., and Adkins, J. F.: A novel  
880 determination of calcite dissolution kinetics in seawater, *Geochim. Cosmochim. Acta*, 170, 51–  
881 68, <https://doi.org/10.1016/j.gca.2015.08.011>, 2015.



- 882 Subhas, A. V., Marx, L., Reynolds, S., Flohr, A., Mawji, E. W., Brown, P. J., and Cael, B. B.:  
883 Microbial ecosystem responses to alkalinity enhancement in the North Atlantic Subtropical Gyre,  
884 *Frontiers in Climate*, 4, <https://doi.org/10.3389/fclim.2022.784997>, 2022.
- 885 Suitner, N., Faucher, G., Lim, C., Schneider, J., Moras, C. A., Riebesell, U., and Hartmann, J.:  
886 Ocean alkalinity enhancement approaches and the predictability of runaway precipitation  
887 processes: results of an experimental study to determine critical alkalinity ranges for safe and  
888 sustainable application scenarios, *Biogeosciences*, 21, 4587–4604, [https://doi.org/10.5194/bg-21-](https://doi.org/10.5194/bg-21-4587-2024)  
889 4587-2024, 2024.
- 890 Sulpis, O., Boudreau, B. P., Mucci, A., Jenkins, C., Trossman, D. S., Arbic, B. K., and Key, R.  
891 M.: Current CaCO<sub>3</sub> dissolution at the seafloor caused by anthropogenic CO<sub>2</sub>, *Proc. Natl. Acad.*  
892 *Sci. U. S. A.*, 115, 11700–11705, <https://doi.org/10.1073/pnas.1804250115>, 2018.
- 893 Traboni, C., Nocera, A. C., Romano, F., Courboulès, J., Chantzaras, C., Magiopoulos, I.,  
894 Varliero, S., Basso, D., and Pitta, P.: Plankton do not care: Minimal effects of ocean liming on  
895 plankton growth and grazing in the Eastern Mediterranean, *Limnol. Oceanogr.*,  
896 <https://doi.org/10.1002/lno.70136>, 2025.
- 897 (UNFCCC) United Nations Framework Convention on Climate Change: NDC Synthesis Report,  
898 2022.
- 899 U.S. EPA: Standard Operating Procedure for In Vitro Determination of Chlorophyll a in  
900 Freshwater Phytoplankton by Fluorescence LG405, 2021.
- 901 Wolf-Gladrow, D. and Riebesell, U.: Diffusion and reactions in the vicinity of plankton: A  
902 refined model for inorganic carbon transport, *Mar. Chem.*, 59, 17–34,  
903 [https://doi.org/10.1016/S0304-4203\(97\)00069-8](https://doi.org/10.1016/S0304-4203(97)00069-8), 1997.
- 904 Zachos, J. C., Röhl, U., Schellenberg, S. A., Sluijs, A., Hodell, D. A., Kelly, D. C., Thomas, E.,  
905 Nicolo, M., Raffi, I., Lourens, L. J., McCarren, H., and Kroon, D.: Rapid Acidification of the  
906 Ocean During the Paleocene-Eocene Thermal Maximum, *Science* (1979)., 308, 1611–1615,  
907 <https://doi.org/10.1126/science.1109004>, 2005.
- 908 Zondervan, I., Zeebe, R. E., Rost, B., and Riebesell, U.: Decreasing marine biogenic  
909 calcification: A negative feedback on rising atmospheric  $p\text{CO}_2$ , *Global Biogeochem. Cycles*, 15,  
910 507–516, <https://doi.org/10.1029/2000GB001321>, 2001.
- 911